

# Calreticulin Enhances Porcine Wound Repair by Diverse Biological Effects

Lillian B. Nanney,<sup>\*†</sup> Christopher D. Woodrell,<sup>‡</sup>  
Mathew R. Greives,<sup>‡</sup> Nancy L. Cardwell,<sup>\*</sup>  
Alonda C. Pollins,<sup>\*</sup> Tara A. Bancroft,<sup>‡</sup>  
Adrienne Chesser,<sup>‡</sup> Marek Michalak,<sup>§</sup>  
Mohammad Rahman,<sup>‡</sup> John W. Siebert,<sup>‡</sup>  
and Leslie I. Gold<sup>‡</sup>

From the Departments of Plastic Surgery\* and Cell and Developmental Biology,<sup>†</sup> Vanderbilt University School of Medicine, Nashville, Tennessee; the Departments of Medicine and Pathology,<sup>‡</sup> New York University School of Medicine, New York, New York; and the Department of Biochemistry,<sup>§</sup> University of Alberta, Edmonton, Alberta, Canada

**Extracellular functions of the endoplasmic reticulum chaperone protein calreticulin (CRT) are emerging. Here we show novel roles for exogenous CRT in both cutaneous wound healing and diverse processes associated with repair. Compared with platelet-derived growth factor-BB-treated controls, topical application of CRT to porcine excisional wounds enhanced the rate of wound re-epithelialization. In both normal and steroid-impaired pigs, CRT increased granulation tissue formation. Immunohistochemical analyses of the wounds 5 and 10 days after injury revealed marked up-regulation of transforming growth factor- $\beta$ 3 (a key regulator of wound healing), a threefold increase in macrophage influx, and an increase in the cellular proliferation of basal keratinocytes of the new epidermis and of cells of the neodermis. *In vitro* studies confirmed that CRT induced a greater than twofold increase in the cellular proliferation of primary human keratinocytes, fibroblasts, and microvascular endothelial cells (with 100 pg/ml, 100 ng/ml, and 1.0 pg/ml, respectively). Moreover, using a scratch plate assay, CRT maximally induced the cellular migration of keratinocytes and fibroblasts (with 10 pg/ml and 1 ng/ml, respectively). In addition, CRT induced concentration-dependent migration of keratinocytes, fibroblasts, macrophages, and monocytes in chamber assays. These *in vitro* bioactivities provide mechanistic support for the positive biological effects of CRT observed on both the epidermis and dermis of wounds *in vivo*, underscoring a significant role for**

**CRT in the repair of cutaneous wounds. (Am J Pathol 2008, 173:610–630; DOI: 10.2353/ajpath.2008.071027)**

Calreticulin (CRT) is a highly conserved major calcium-binding protein of the endoplasmic reticulum (ER). Whereas extracellular functions of CRT are constantly emerging, the heralded functions of CRT are intracellular, in calcium homeostasis and in binding N-linked oligosaccharide protein intermediates to ensure proper glycoprotein conformation in the ER.<sup>1–4</sup> CRT has an amino terminal signal sequence, a carboxy terminal KDEL ER retrieval sequence, multiple calcium-binding sites and harbors three distinct domains N, P, and C within its 46,000-da molecular mass (400 amino acids).<sup>5</sup> Importantly, the release of calcium from the ER regulates multiple calcium-driven intracellular signaling pathways and protein actions.<sup>2</sup>

Novel extracellular functions of CRT continue to be unraveled, portraying a protein with strong impact on developmental, physiological, and pathological processes.<sup>2,3</sup> CRT has been localized to the surface of a variety of cells including platelets, fibroblasts, apoptotic cells, and endothelial cells. However, it is not clear whether CRT on the cell surface is derived exogenously (from neighboring cells or the circulation) and/or from within the cell. CRT has been considered as a stress response protein that is up-regulated following injury<sup>6</sup> and hypoxia,<sup>2</sup> which exist in the wound environment.<sup>7–9</sup> Although the mechanism(s) by which CRT exits the cell are unclear, stress or injury-related release of this protein may be a requisite step in the physiology of wound repair.

Biological activities of CRT that can be considered extracellular are largely related to cellular adhesion, migration, and phagocytosis; all are critical aspects of wound healing. For example, CRT binds to the cytoplas-

---

Supported by Calretex, LLC (L.B.N. and L.I.G.) and National Institutes of Health grants GM40437 and P30 AR41943 (to L.B.N.).

Accepted for publication May 29, 2008.

Parts of this work were presented at the 14th and 15th annual meetings of the Wound Healing Society and at the sixth and seventh International Workshops on Calreticulin.

Address reprint requests to Leslie I. Gold, Ph.D., New York University School of Medicine, Departments of Medicine and Pathology, 550 First Avenue NB16S13, New York, NY 10016. E-mail: leslie.gold@nyuma.org.

mic tail of  $\alpha$  integrins, acting as an escort through the ER, and maintains appropriate calcium balance for integrin signaling and adhesion-dependent functions of matrix proteins with significant impact on regulating cell shape, motility, and spreading.<sup>10-12</sup> In addition, the integrin-binding basement membrane protein, laminin, interacts with CRT to mediate migration.<sup>13,14</sup> The concentration-dependent calcium-binding as well as the zinc and ATP-binding ability of CRT are important in maintaining proper conformation of the molecule for function within the ER<sup>15</sup> and likely its extracellular functions as well. Both overexpression of CRT and CRT deficiency affect matrix protein expression, such as fibronectin, and cell adhesion and spreading related to integrin function.<sup>16-18</sup> An increase in vinculin and N-cadherin and a decrease in tyrosine phosphorylation of  $\beta$ -catenin are other adhesion related proteins/events that CRT is deemed to regulate from the ER in a calcium-dependent manner.<sup>2,19,20</sup>

Apart from the recognized inside-out cellular signaling, CRT has been shown to engage in outside-in signaling through its presence on the cell surface.<sup>21-26</sup> As a cell surface protein without signaling capability, CRT has been shown to bind to the promiscuous low-density lipoprotein receptor-related protein (LRP/CD91/ $\alpha$ -2 macroglobulin receptor) and to thrombospondin-1 (TSP-1), a protein engaged in actin cytoskeletal and focal adhesion reorganization.<sup>22</sup> Together, as a signaling complex, CRT, TSP-1, and LRP mediate focal adhesion disassembly, important in the migratory process. Accordingly, both CRT-null and LRP-null fibroblasts lose their migratory response to TSP-1. A role for CRT in immune cell function is implicated by its ability to act as a cell surface coreceptor for C1q<sup>27</sup> and in activating human neutrophils. CRT is also up-regulated in the granules of cytotoxic T lymphocytes.<sup>3,28</sup> Interestingly, CRT on the surface of apoptotic cells engages the LRP receptor on phagocytic cells as a requirement for their uptake and removal.<sup>26</sup> A concurring recent study shows that apoptotic cancer cells are immunogenic and induce phagocytic uptake on either exogenous addition of CRT or by induction of its translocation to the cell surface.<sup>29</sup>

Normal wound healing is a dynamic process that encompasses three essential phases after clot formation.<sup>30-32</sup> The first is an inflammatory phase, which commences with leukocytes and macrophages migrating into the wound to phagocytose bacteria and remove dead tissue/cells (debridement). Within 1 to 2 days after injury, keratinocytes proliferate at the wound margins before starting to migrate over the wound. Keratinocytes in the hair follicles and sweat ducts begin migrating upward also to resurface the wound. The subsequent proliferative or tissue formation phase is aided by cytokines and growth factors, including transforming growth factor (TGF)- $\beta$ , FGF, vascular endothelial growth factor (VEGF), and platelet-derived growth factor (PDGF), secreted by macrophages that attract fibroblasts, connective tissue cells, and endothelial cells from the periwound stroma. Release of cytokines continues with participation from the cells that have newly arrived to the wound and from the epidermal cells. In addition, the dermal cells produce extracellular matrix proteins, such as collagens, to fill in the wound defect and provide a provisional matrix (granulation

tissue) for the continued migration of keratinocytes to re-epithelialize the wound. A continued influx of macrophages and fibroblasts providing growth factors for neovascularization and matrix deposition in the wound bed, and proteases for clot dissolution and tissue remodeling, proceeds beyond wound closure. Thus, numerous cell types and processes must stochastically interact to bring about cutaneous repair.

Over 7 million people in the world develop chronic non-healing wounds related to different causes, including pressure ulcers, venous stasis ulcers, and diabetic neuropathy leading to chronic foot ulcers.<sup>30</sup> As the prevalence of diabetes, largely related to the surge in obesity, is 7% of the United States population (approximately 21 million in 2005), the morbidity of defective wound healing, the most critical being amputation, has become a serious problem requiring novel therapies/agents to improve wound healing rate and quality. CRT was originally shown to be the biologically active component of a hyaluronic acid isolate from fetal sheep skin that accelerated wound healing in animal experimental models of cutaneous repair.<sup>33-35</sup> In consideration of potential candidates for targeted therapy for impaired wound healing, the present study was undertaken to determine whether CRT treatment could sufficiently improve wound healing in a porcine model of wound repair. This paradigm of tissue repair has been used to demonstrate the efficacy of various wound healing treatments, because this animal model most closely mimics human wound healing.<sup>36,37</sup> For example, porcine and human skin share similar epidermal and dermal-epidermal thickness ratios, mosaic hair growth, and have similar hair and blood vessel distribution. To approach the problem of defective wound healing posed by diseases such as diabetes, we also sought to determine whether CRT would enhance repair in steroid-treated pigs, as a model of impaired wound healing. Moreover, since the mechanisms involved in the ability of CRT to enhance wound repair are unknown, we sought to interrogate the biological effects that enable CRT-mediated repair.

Our studies show that topical application of CRT to partial thickness porcine wounds positively affects both epidermal and dermal aspects of cutaneous wound repair. In general, the CRT-treated wounds show an increase in the rate of re-epithelialization and a greater degree of stratification of the epidermal layer and amount of granulation tissue, reaching wound maturity earlier than PDGF-BB-treated wounds, used as positive control. Similar positive effects are observed in the dermis of the CRT-treated wounds of steroid-treated pigs. Furthermore, in the CRT-treated wounds, TGF- $\beta$ 3, an important protein in driving matrix formation and inducing cellular migration, including the influx of macrophages into the wounds, is markedly increased in the dermis. In addition, the CRT-treated wounds show a comparatively remarkable increase in proliferating basal keratinocytes and cells of the neodermis. The effects demonstrated *in vivo* are substantiated by *in vitro* bioactivities showing that CRT stimulates proliferation and migration of cells critical to both wound resurfacing and remodeling.

## Materials and Methods

### Materials

Recombinant rabbit calreticulin (from M. Michalak University of Alberta, Edmonton Alberta, Canada), expressed in *Escherichia coli* as a his-tagged protein that was purified to homogeneity by nickel-Sepharose chromatography, was shown to be properly folded and migrated as a single band at  $M_r$  50,000 by sodium dodecyl sulfate-polyacrylamide gel electrophoresis, as described.<sup>39</sup> Human CRT was obtained from GenWay Biotech (10-288-22432F; San Diego, CA). CRT was stored in 10 mmol/L Tris containing 3.0 mmol/L calcium, pH 7.0 (termed buffer), to maintain proper conformation of this calcium-binding molecule. Anti-peptide antibodies (purified IgG) specific for each isoform of TGF- $\beta$  (TGF- $\beta$ 1, TGF- $\beta$ 2, and TGF- $\beta$ 3) have previously been described.<sup>39</sup> Isoform-specific cytokeratin 14 antibody was obtained from Accurate Scientific (Westbury, NY). Goat anti-calreticulin (pantropic; BIOCAN/Jackson Immunochemicals) was a gift from Marek Michalak (University of Alberta). Rabbit anti-human Kinetichore nuclear protein (KI-67) was from Nova Castra Laboratories Ltd. (Newcastle, UK) and a monoclonal mouse anti-human antibody specific for macrophages (MAC387) was purchased from Serotec, Ltd, Raleigh, NC).

### Porcine Wound Models and Treatments

Adolescent Yorkshire pigs weighing approximately 50 to 60 lb were housed, fed, and treated in accordance with protocols approved by the Institute Animal Care and Use Committee at Vanderbilt University Medical Center. Before surgery, animals were anesthetized with a mixture of ketamine (2.2 mg/kg), Telazol (4.4 mg/kg) and xylazine (2.2 mg/kg) by intramuscular injection, subsequently intubated and maintained on inhalation of oxygen and isoflurane. Cefazolin antibiotic was administered intramuscularly immediately before surgery and was given orally on subsequent days. In preparation for surgical excision, the dorsal surface of the pig was clipped, shaved from shoulder to flank, and disinfected with Betadine soap. In a sterile manner, four longitudinal partial thickness wounds were created along the paravertebral region to a depth of 1560  $\mu$ m with a Zimmer dermatome (Warsaw, IN). A series of individual 1.5  $\times$  1.5 inch nonmeshed skin graft bridges secured with staples separated the area into individual excisional partial thickness wounds. CRT at 1.0 mg/ml and 5.0 mg/ml was topically applied to the wounds and the treated wound tissue harvested at 5 and 10 days after wounding. To enable harvesting the wounds at the same time, the wounds were made in a reverse order. Accordingly, one-half of the wounds were created at the onset of the experiment, and the remaining wounds were created 5 days later, so that each animal was euthanized on the 10th day following initial wounding ( $n = 6$  wounds/parameter studied). The commercially available wound healing agent, Regranex (0.01% PDGF-BB; Ethicon, Inc., Somerville, NJ) gel formulation was used as positive control. Two wounds/treatment group/pig were used. To prevent roll-off of the liquid, 0.05 ml of CRT or buffer was applied to the animal lying on its side and the wound dried for 1 minute before applying a K-Y gel formu-

lation for the maintenance of moist wound healing conditions. The wounds were covered and protected with Op-Site semioclusive bandages. Each wound was cleansed daily with saline and bandages replaced. Buprenex (intramuscular) was used for analgesic control during the initial postoperative period. To ensure sustained analgesic control, animals received 25  $\mu$ g/hour Duragesic patches for 3 days (fentanyl transdermal system). Topical treatments of CRT and buffer controls were repeated daily for the first 4 days; PDGF-BB was applied once at the time of wounding, since in standard protocols this drug is not recommended for daily dosage. To control for possible effects of wound location on the rate of healing, wound placement patterns from the various treatment groups were randomized.

For steroid-impaired wound healing, 48 hours before the creation of the wounds, pigs were administered an intramuscular injection of 1 mg/kg dose of methylprednisolone acetate (Depo Medrol; Henry-Schein, Melville, NY) and the wounds prepared and treated as described above. Treatment groups were the same for both the normal and impaired wound healing models. Animals were euthanized and tissues collected for study after 6 days (two pigs) or 7 days (one pig) of healing; the wounds were completely re-epithelialized at these time points.

### Histological Preparation and Morphometric Analysis

At the termination time for each experiment, wounds with an adjacent margin of normal skin were excised, divided vertically into three full-thickness tissue sections/wound, fixed in 10% neutral buffered formalin for 24 hours, embedded in paraffin, and 5.0- $\mu$ m-thick tissue sections mounted on glass slides for histological analysis and immunohistochemistry. The tissue sections were stained as described below and the extent of re-epithelialization and dermal depth (granulation tissue formation) of the wounds determined by morphometric analysis. Serial images of wounds were captured under a light microscope and displayed on a video screen using an Olympus model AHBT camera. Quantitative measurements were performed using Image-Pro Plus scientific image analysis software (Media Cybernetic, Inc., Silver Spring, MD.).

### Re-Epithelialization

The wounds of the normal pigs were used to assess re-epithelialization. Antibodies to cytokeratin 14 were used to selectively highlight the newly resurfaced epithelial islands and epidermal margins. The extent of re-epithelialization of the wounds was determined on wounds after 5 days of healing in the normal pigs by measuring a composite of newly resurfaced epidermis that migrated over the wounds from the wound edges and epithelial islands derived from surviving epithelium that migrated upward from hair follicles and sweat ducts, compared to the total wound length. The data are expressed as a percentage of resurfacing as described.<sup>40</sup>

### *Granulation Tissue/Neodermal Depth Assessment*

Granulation tissue thickness was measured in trichrome-stained tissue slides, extending from the non-re-epithelialized surface of the granulating wound down to its intersection with the underlying unwounded dermis. The granulation tissue becomes converted into a neodermis as re-epithelialization is nearly complete, which is measured as dermal depth. Dermal depth measurements extend from the dermal-epidermal junction down to the intersection of the newly formed granulation tissue with the adjacent underlying unwounded dermis of these partial thickness wound beds. To determine the average thickness of the granulation tissue at 5 days of healing or dermal depth, at 10 days of healing in the normal pigs, and 6 to 7 days in the steroid-challenged pigs, five or more random areas were measured in micrometers as described.<sup>40</sup> Data are expressed as means  $\pm$  SEM.

### *Assay for Wound-Breaking (Tensile) Strength*

The effect of CRT on wound breaking strength was performed using a rat incisional model as described.<sup>41</sup> Four full-thickness linear incisional wounds (3 cm in length) were created in the dorsal skin of each rat. After hemostasis was achieved, the edges of the wounds were approximated with EX clips (Bainbridge Scientific, Bainbridge, MA) and the wound incisions on each animal were treated with CRT at 5.0 mg/ml and 10 mg/ml, buffer alone or Regranex. The rats were sacrificed at 7, 14, 21, and 28 days ( $n = 10$  rats/parameter/time point). Strips of skin, 1.0 cm  $\times$  5.0 cm in length, perpendicular to the incision line were clamped into an Instron tensiometer (Canton, MA) and tensile strength (breaking strength/cross-sectional area) was determined.

### *Immunohistochemistry*

#### *Calreticulin Expression*

The temporal and spatial expression of CRT during wound healing was determined at 5 and 10 days of healing by immunohistochemical localization using a polyclonal goat anti-CRT. The slides were baked overnight at 56°C and passed through graded alcohol with the final concentration being 30% ethanol. The slides were placed in Tris-buffered saline containing 0.3% Triton X-100 for 15 minutes, followed by 100% methanol for 1 minute, and then peroxidase activity was quenched with 0.6% H<sub>2</sub>O<sub>2</sub> for 30 minutes, followed by 100% methanol for 1 minute. The tissues were blocked with normal rabbit serum (S5000; Vector Laboratories, Burlingame, CA) in Tris-buffered saline containing 0.5% bovine serum albumin (blocking buffer) for 20 minutes at room temperature. The CRT antibody, diluted at 1:1000 in blocking buffer, was incubated with the slides overnight at 4°C *in humido*. After washes with Tris-buffered saline containing 0.1% bovine serum albumin, biotinylated rabbit anti-goat IgG secondary antibody (Vector, BA5000) was applied to the slides for 1 hour at room temperature. The slides were washed and then incubated with ABC reagent (Vec-

tastain kit PK6200) for 1 hour. After rinsing, the slides were dipped in the substrate 0.05% 3,3-diaminobenzidine HCl (DAB; Sigma Chemical D5637) solution until a brown color appeared, counterstained with hematoxylin (Fisher CS401-1D), dehydrated through increasing concentrations of alcohol, and mounted with Permount (Fisher, SP15-100).

#### *TGF- $\beta$ Isoform Expression*

To determine whether TGF- $\beta$  isoform expression was induced in CRT-treated wounds, tissue slides were incubated separately with antibodies to TGF- $\beta$ 1, TGF- $\beta$ 2, and TGF- $\beta$ 3. The antiserum was produced in rabbits to individual peptides of each isoform and the IgG purified by peptide affinity chromatography as described.<sup>42</sup> Slides were treated as described above, except before blocking with goat serum (Vector Laboratories, S-1000), the tissue sections were treated with hyaluronidase (1.0 mg/ml; Sigma Chemical) in sodium acetate, pH 5.0, containing 0.85% NaCl for 1 hour at 37°C. Sections were then incubated overnight with 2.5  $\mu$ g/ml anti-TGF- $\beta$  isoform antibodies, incubated with biotinylated goat anti-rabbit secondary antibody (Vectastain kit Vector Laboratories), and staining continued as described above.

#### *Ki-67 Immunoreactivity*

Actively proliferating cells in the epidermis and neodermis were immunostained for Ki-67 antigen. The tissue slides were subjected to antigen retrieval. Endogenous peroxidase activity was neutralized with 6% H<sub>2</sub>O<sub>2</sub> for 20 minutes followed by blocking nonspecific reactivity with a casein-based protein block (DAKO, Carpinteria, CA) for 10 minutes. The slides were incubated with rabbit anti-human Ki-67 (NovaCastra Laboratories Ltd., Newcastle, UK) diluted at 1:1400 for 60 minutes in Tris-buffered saline. The rabbit Envision HRP system (DAKO) was used with DAB as substrate and the slides counterstained with hematoxylin.

#### *Macrophage Detection*

Macrophage infiltration into the wounds was assessed by immunostaining using a specific antiserum for tissue monocytes/macrophages (MAC.387, AbD; Serotec). The tissue sections underwent antigen retrieval by boiling the slides in 0.01 mol/L Tris-HCl, pH 10. Both quenching peroxidase activity and blocking nonspecific immunoreactivity were performed as described above. A monoclonal mouse anti-human antibody to a macrophage epitope (MAC387) was used at 1:1000 for 1 hour. The mouse Envision HRP System kit (DAKO) was used for detection as described above.

### *In Vitro Effects of Calreticulin*

#### *Cell Cultures*

Primary adult human epidermal keratinocytes (CC-2501; Cambrex-Lonza, Inc., Walkersville, MD) were cul-

tured in keratinocyte growth medium containing additives from the BulletKit (Singlequots) (CC-4131; Cambrex-Lonza), including gentamicin-1000 (Lonza). The cells were subcultured at 50% confluency by washing with 30 mmol/L HEPES-buffered saline, treating with trypsin-EDTA (0.025% trypsin- 0.02% EDTA; Cambrex-Lonza), and neutralizing the trypsin with neutralizing solution (TNS; Lonza). Following slow centrifugation, the cells were resuspended in fresh medium and seeded at different cell densities depending on the experiments described below. Primary human low passage foreskin fibroblasts (CCD 1070SK; American Type Culture Collection, Manassas, VA) were grown in complete Eagle's minimal essential medium (MEM; Gibco/Invitrogen, Carlsbad, CA) containing 10% fetal bovine serum (FBS; HyClone, Logan, UT), 2 mmol/L glutamine (Mediatech, Manassas, VA), and antibiotic-antimycotic (ABAM; Mediatech). At 60 to 70% confluency, the cells were washed with phosphate-buffered saline (PBS), removed for replating with 0.25% trypsin-2.21 mmol/L EDTA (Mediatech), the trypsin neutralized with 10% FBS in MEM, and the cells centrifuged and resuspended in complete MEM at the cell densities described in the assays below. Human dermal microvascular endothelial cells (Cambrex-Lonza) were cultured in complete endothelial cell growth medium (EGM; Lonza) supplemented with the EGM-MV BulletKit (CC-3125; Lonza). The cells were subcultured when approximately 70% confluent by washing with HEPES buffered saline solution, treating with 0.025% trypsin-0.01% EDTA, followed by neutralization with TNS, and the cells then centrifuged and resuspended in complete medium. The human monocyte cell line, THP-1 (American type Culture Collection TIB-202), was cultured in suspension in RPMI 1640 medium (GIBCO/Invitrogen) supplemented with 10% FBS, 1% L-glutamine, and 1% penicillin-streptomycin. The cells were grown by removing medium from the cells and replenishing with fresh medium every 3 to 4 days. The THP-1 monocytes, at a concentration of  $5 \times 10^5$ /ml in 10 ml of complete medium, were differentiated into macrophages by the addition of phorbol myristate acetate at 10 ng/ml for 48 hours.

### *Cellular Proliferation*

The primary human keratinocytes were seeded in 96-well tissue culture plates at a density of  $2.0 \times 10^3$  cells/well in keratinocyte growth medium and incubated for 48 hours or until the cells reached 50–60% confluency. The cells were washed with keratinocyte basal medium (KBM, Cambrex-Lonza) and treated with increasing concentrations of CRT (0–200 pg/ml) in KBM in triplicate. In certain experiments, keratinocytes were synchronized by growing in KBM for 24 hours before treating. Human epidermal growth factor (EGF) (10 ng/ml; Invitrogen, Carlsbad, CA) was used as a positive control, and KBM served as a negative control. After 72 hours, metabolic activity as a reflection of cell growth was determined using the Cell-Titer 96 AQueous One Solution cell proliferation assay (G3580, Promega, Madison, WI). The absorbance of the soluble formazan chromophore was quantitated after 2 hours using a microplate reader (BioRad 680) at a wave-

length of 490 nm. The primary human dermal fibroblasts in complete MEM were seeded in 96-well tissue culture plate at a cell density of  $2.0 \times 10^3$  cells/well. At approximately 50% confluency (approximately 48 hours), the cells were switched to MEM containing 0.5% serum for 24 hours, treated with increasing concentrations of rabbit or human CRT (0–200 ng/ml) in triplicate for 72 hours, and cellular proliferation assessed by the MTS assay. Human fibroblast growth factor (FGF) (5.0 ng/ml; R & D Systems, Minneapolis, MN) and MEM containing 0.5% serum were positive and negative controls, respectively. Primary human microvascular endothelial cells were seeded in 96-well plates at a cell density of  $2 \times 10^3$ /well in complete EGM. On reaching approximately 60% confluence, the cells were switched to basal EGM containing 0.5% serum overnight and then increasing concentrations of CRT (0–50 pg/ml) were added and cellular proliferation assessed by the MTS assay after 24 hours. VEGF (10 ng/ml; Genway Biotech, San Diego, CA), and basal EGM were positive and negative controls, respectively. The concentrations of CRT described for each of the three cell types were predetermined by initially using a wider range of doses.

### *Wound Healing Scratch Plate Assay*

The primary human keratinocytes and dermal fibroblasts were seeded in 24-well tissue culture plates at  $2.0 \times 10^4$ /well and  $1.0 \times 10^4$ /well, respectively, in their respective complete media and the cells grown to approximately 70 to 80% confluence. The keratinocytes were washed with KBM and incubated in KBM for 18 hours before wounding. Wounds were created in each well by drawing a line down the center of the well with a 200- $\mu$ l plastic pipette and the plate washed with KBM or serum-free MEM to remove the displaced cells. To denote the edges of the original wound, a dot was marked with a black pen on the underside of the plate. Following washing with medium, increasing concentrations of CRT in KBM or MEM were added to keratinocytes (0–100 pg/ml) and to fibroblasts (0–10 ng/ml), respectively, in duplicate wells. Human EGF (10 ng/ml) and 5% FBS were used as positive control for keratinocytes and fibroblasts, respectively. Negative controls were KBM for keratinocytes and MEM for fibroblasts. After 48 and 24 hours incubation for the keratinocytes and fibroblasts, respectively, the cells were stained with 0.025% Coomassie blue in 10% acetic acid–45% methanol for 10 minutes and washed twice with PBS or water. The wells were viewed with an inverted light microscope (Axiovert S-100; Zeiss, Thornwood, NY) and images captured using Metamorph software (Molecular Probes, Eugene, OR). Wound closure (cellular migration) was determined using National Institutes of Health Image J version 1.37 software by outlining the front of cell migration into the wounds, calculating the area of the scratch remaining unoccupied by the cells and comparing this area to area in the original scratch at time 0. Alternatively, percent wound closure (migration) of the wound was determined by counting the number of cells in 16 rectangles of set dimensions that had migrated over the line of the original wound at time 0 using Image J software.

### Thin Membrane Chamber Cellular Migration Assays

A thin-membrane ChemoTx system (Neuroprobe Inc., Gaithersburg, MD) in a 96-well plate format and two different cell-labeling methods were used to determine whether CRT mediates directed migration of keratinocytes, fibroblasts, monocytes, and macrophages. The assay was performed according to the manufacturer's instructions. Fibroblasts and adherent macrophages were washed with PBS and removed from the plate with 0.25% trypsin–2.21 mmol/L EDTA in Hanks' balanced salt solution (HBSS; Cellgro, Herndon, VA), the trypsin activity neutralized with serum-containing medium, and the cells centrifuged at  $235 \times g$  for 5 minutes. Keratinocytes were washed with HEPES-BSS (Lonza, Walkersville, MD) and trypsinized, suspended in TNS, and centrifuged as described above. All cell pellets were suspended in their respective serum-free media. The migration wells in the bottom chamber were loaded with 330  $\mu\text{l}$  of increasing dilutions of CRT in serum-free medium for keratinocytes, fibroblasts, monocytes, and macrophages. Treatments were performed in triplicate. Serum-free medium was used as a negative control and EGF (10 ng/ml; keratinocytes), FGF (5.0 ng/ml; fibroblasts), the phlogistic agent, *N*-formyl-Met-Leu-Phe (fMLP, 1–100 nmol/L, monocytes; Sigma Chemical Co, St. Louis, MO), and VEGF (100 ng/ml; Fisher Scientific) or fMLP (100 nmol/L macrophages) were used as positive controls, as shown in individual experiments. The frame of the apparatus containing the membrane was carefully placed on top of the wells, 50  $\mu\text{l}$  of cell suspension was loaded onto the membrane above each well bordered by a rubber gasket, the lid replaced, and the cells incubated at 37°C, 5% CO<sub>2</sub>. The number of cells/well, pore size of the polycarbonate Neuroprobe membrane, and migration time period varied for each cell type as follows: keratinocytes at  $2.5 \times 10^4$ /well, 8  $\mu\text{m}$  pore size, 4 hours; fibroblasts at  $5.0 \times 10^4$ /well, 8.0  $\mu\text{m}$ , 4 hours; THP-1 monocytes at  $5 \times 10^4$ /well, 5  $\mu\text{m}$  pore size, 1 hour; THP-1 macrophages at  $2.5 \times 10^4$ /well, 5.0  $\mu\text{m}$  pore size, 2 hours. Following the respective incubation periods, the chambers were dismantled, the membranes washed with PBS, the cells fixed with 4% paraformaldehyde for 5 minutes, and the membranes applied to coverslips, which were sealed and stained using VECTASHIELD and 4,6-diamidino-2-phenylindole (DAPI) (Vector Laboratories). Each membrane was photographed at 200 $\times$  magnification in at least 6 fields, and an average of 3 high-power fields were calculated for the number of cells/well using Kodak ID software. In certain experiments, the THP-1 monocytes and phorbol 12-myristate 13-acetate-induced differentiated adherent macrophages were labeled with 2 to 4  $\mu\text{mol/L}$  calcein AM (Molecular Probes, Eugene, OR) before applying the cells to the membrane. The concentration of the fluorochrome and incubation times varied for each cell type as follows: macrophages, 4  $\mu\text{mol/L}$  calcein for 30 minutes; monocytes, 2  $\mu\text{mol/L}$  calcein for 40 minutes. Following the incubation times, the remaining cell suspension was aspirated, the membrane carefully wiped with a cotton swab dipped in PBS, treated with 20  $\mu\text{M}$  EDTA in PBS for 20 minutes at 4°C and the plate centrifuged at 1500 rpm (Beckman model J-6M, Fullerton, CA) for 10 minutes at 4°C to detach the cells in the membrane into the lower chamber. The membrane

was removed and fluorescence reflecting the number of cells that migrated in and through the membrane into the bottom chamber was determined in a fluorimeter (Victor 3V multilabel counter, Perkin Elmer, Waltham, MA) using excitation and emission wavelengths of 485 nm and 535 nm, respectively.

### Statistical Analyses

For the morphometric analyses of the wounds, the values obtained were subjected to the Kruskal-Wallis test for nonparametric samples. A Mann-Whitney test was used for comparison between individual samples. Statistical analyses for all experiments were performed using SPSS version 12 software (Chicago, IL).

## Results

### CRT Enhances Porcine Wound Healing

An accelerated rate of wound re-epithelialization of wounds is one of the indicators of enhanced wound repair. After 5 days of healing, epithelial islands and epithelial wound edges in CRT-treated wounds display a higher degree of resurfacing and epidermal stratification compared to either the wounds treated with buffer or PDGF-BB (not shown). Regranex (PDGF-BB), the first and only Food and Drug Administration-approved cytokine (protein) treatment for cutaneous wound repair, was used as a positive control in the wound healing experiments.<sup>30,43,44</sup> The percentage of epithelial resurfacing (percent re-epithelialized) with 5.0 mg/ml CRT (100  $\mu\text{g/wound}$ ) was 58% compared to 41% and 44% for the PDGF-BB-treated and buffer-treated wounds, respectively, at 5 days after injury (Figure 1A). As shown, by 10 days after wounding, the CRT-treated and control wounds were 100% re-epithelialized (Figure 2, A, B, D, E). Both the increase in re-epithelialization of the CRT-treated wounds at 5 days (Figure 1A) and the higher degree of stratification and cornification at 10 days (Figure 2, A and D) suggest that CRT increased the rate of epidermal maturity. Quantitative analysis of epithelial resurfacing, based on six wounds/treatment group, revealed a trend as shown by the graph in Figure 1A but fell short of reaching statistical significance ( $P \leq 0.058$ ). From the histological observations (compare Figure 2, A and D, to C and F) and the trend from the quantitative data set, it appears that statistical significance might have been achieved with a larger number of wounds/group that was not feasible in this study due to lack of sufficient supply of CRT for the large animal wounds.

### Granulation Tissue Formation/Neo-Dermal Depth

Restoration of dermal tissue is a dynamic process essential for remodeling the wound bed. The accrual of neo-dermal connective tissue is largely mediated by fibroblasts recruited into the wound, the continued migration, proliferation, and production of extracellular matrix proteins by these cells, capillary ingrowth, and an influx of

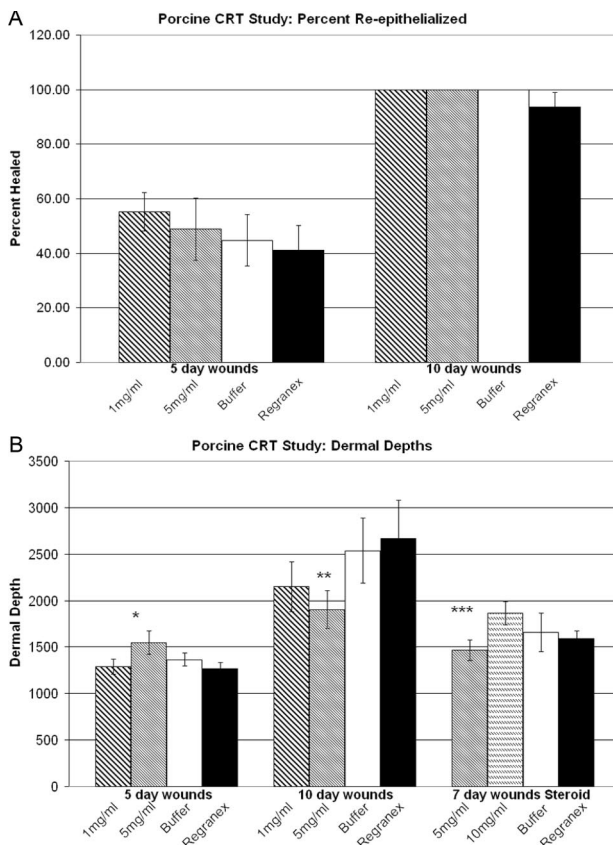


**Figure 1.** Graphs of quantitative morphometric analysis of CRT-treated porcine wounds at 5 and 10 days after injury. **A:** Re-epithelialization expressed as percent healed of wounds in normal pigs after 5 days and 10 days of healing. The exogenously applied treatments are: 1.0 mg/ml or 5.0 mg/ml CRT, buffer or PDGF-BB. 5 days after wounding, CRT induced a trend toward enhancing re-epithelialization (resurfacing) of the wounds ( $P = 0.58$ ;  $n = 6$  wounds/parameter). By 10 days after wounding, only the PDGF-BB-treated wounds were not 100% re-epithelialized. The percent healed is presented as the mean  $\pm$  SEM. **B:** Granulation tissue/neodermal depth measurements of treated (as in **A**) wounds in normal pigs show that after 5 days of healing, CRT induced a dose-dependent increase in dermal thickness ( $*P \leq 0.058$ ;  $n = 4$ ). At 10 days of healing, the dermal depths of the 5.0 mg/ml CRT-treated wounds were significantly smaller than the buffer ( $**P \leq 0.05$ ;  $n = 6$ ) and PDGF-BB-treated wounds ( $**P \leq 0.04$ ;  $n = 6$ ), reflecting the more advanced healing observed by the histology of the CRT-treated wounds (compare Figure 2, A and D, with C and F). In the steroid-impaired wounds, a dose-dependent response was obtained with 5.0 mg/ml and 10 mg/ml CRT at 7 days after wounding ( $***P \leq 0.034$ ;  $n = 6$ ). The dermal depths are presented as the mean  $\pm$  SEM.

inflammatory cells and progenitor cells from outside the confines of the wound.<sup>32,45</sup> The extent of matrix formation is a composite assessment reflecting the quality of the dermal response. Early in the reparative process, before the epidermis heals across the wound surface, the wound bed is filled with a loose granulation tissue sparsely populated with cells, which progressively forms a mature, comparatively dense, irregular connective tissue containing increasing amounts of collagen.

In wounds examined 5 days after wounding, the neodermal depth (granulation tissue) was thicker in the 5 mg/ml compared to 1.0 mg/ml CRT-treated wounds (Figure 1B;  $*P \leq 0.058$ ). Surprisingly, the higher dose of CRT induced a statistically significant greater neodermal depth than PDGF-BB (Figure 1B;  $*P < 0.04$ ). By 10 days of healing, there was a dose-dependent compaction of

neodermal depth in the 1.0 mg/ml and 5.0 mg/ml CRT-treated wounds, which was statistically significant compared with the buffer and PDGF-BB-treated wounds (Figure 1B;  $**P \leq 0.05$  and  $P \leq 0.04$ , respectively). Similar to the greater degree of epidermal maturity, marked by epidermal stratification of the CRT-treated wounds (Figure 2, A and D) compared to the buffer (Figure 2, B and E) and PDGF-BB-treated wounds (Figure 2, C and F), the decrease in dermal depth in the CRT-treated wounds represents a neodermis that is found later in the wound repair process. These more mature wounds show a characteristic notable uniform distribution of collagen fibers throughout the neodermis (Figure 2, A, D, G). The less mature PDGF-BB-treated wounds have equally dense collagen in the deepest regions of the dermis but less collagen density near the top of the wound bed where the epidermis has not quite resurfaced the wound (Figure 2, C, F, I).

Steroid-treatment of pigs is a well-established model for impaired healing. Since the effects are generally mediated through macrophages with effects observed on collagen synthesis, this model is more useful for detecting effects in the dermis and thus is applicable to events that frequently impair human healing.<sup>46</sup> In steroid-challenged pigs, the wounds were harvested after 7 days of healing. On histological examination, re-epithelialization of the wounds was 100% complete, thereby obviating the ability to determine the effect of the treatments on rate of wound resurfacing. However, measurement of neodermal depths show that the 5.0 mg/ml CRT- and PDGF-BB-treated wounds were nearly equal (Figure 1B) and a dose-dependent effect in dermal depth was achieved with 5.0 mg/ml and 10.0 mg/ml CRT (Figure 1B;  $***P \leq 0.034$ ). Although CRT at 10 mg/ml induced a greater dermal depth than the buffer and PDGF-BB controls, this apparent trend representing a small number of wounds was not statistically significant.

### Calreticulin Increases Wound Tensile Strength

The quantitative (Figure 1) and qualitative (Figure 2) effects of CRT on the granulation tissue/neodermis suggested that the CRT-treated wounds might have greater integrity of wound strength compared to the buffer and PDGF-BB-treated wounds. Therefore, we analyzed the impact of CRT on the wound tensile strength using a well-established rat incisional model for wound breaking tensile strength.<sup>41</sup> Using this assay, CRT at 5.0 mg/ml after 21 days induced a statistically significant increase in the breaking strength of the wounds compared to the buffer or the PDGF-BB-treated wounds (Figure 3;  $*P \leq 0.019$ ). The specificity of this biological response was substantiated by an even greater breaking strength of wounds treated with 10 mg/ml CRT compared to both the buffer ( $*P \leq 0.001$ ) and PDGF-BB-treated wounds ( $**P \leq 0.027$ ). Wounds harvested at 7, 14, or 42 days of healing did not show statistically significant differences in breaking strength among the various treatment groups (Figure 3).

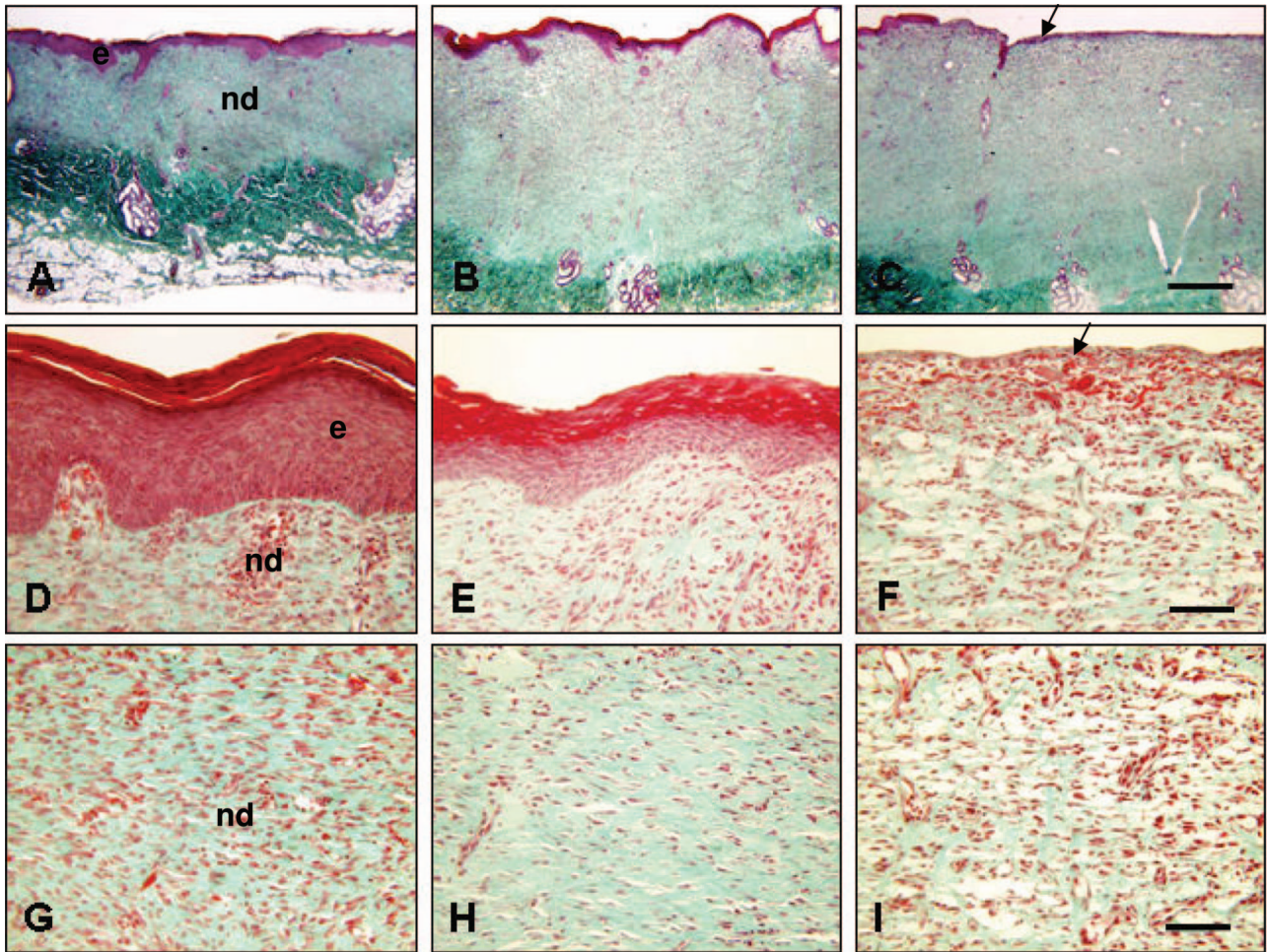


**Figure 2.** Micrographs of trichrome-stained CRT-treated porcine wounds after 10 days of healing. Treatments were 5.0 mg/ml CRT (**A, D, G**); buffer (**B, E, H**); PDGF-BB (**C, F, I**). Treatment with CRT resulted in a more mature stratified epidermis (**A, D**) as compared to buffer-treated (**B, E**) and PDGF-BB-treated wounds (**F, I**). In addition to the more stratified epidermis in the CRT-treated wounds (**D**), the neodermis of these wounds (**A**) is much more compacted than the buffer-treated (**B**) and PDGF-BB-treated (**C**) wounds. Thus, both the epidermis and dermis of the CRT-treated wounds (**A, D, G**) represent a higher degree of maturity than either the buffer-treated (**B, E, H**) or PDGF-BB-treated (**C, F, I**) wounds. Scale bars: **A-C** = 850  $\mu$ m; **D-I** = 88  $\mu$ m. Cells are stained red and collagen cyano-blue. e, epidermis; nd, neodermis.

### *CRT Is Dynamically Expressed during Wound Repair*

A dynamic expression of CRT during wound repair would suggest a physiological role for this protein in tissue repair. Moreover, the fact that exogenously applied CRT exerted apparent effects on both the epidermal and dermal components of the porcine partial thickness wounds supports this idea. Therefore, we evaluated the spatial and temporal distribution of endogenous CRT in the wound repair models by immunohistochemistry. In unwounded (adjacent) skin, basal and suprabasal keratinocytes layers of normal skin show slight to no immunoreactivity in contrast to the more differentiated stratum corneum, granulosum, and spinosum upper layers of epidermis, which show intense immunoreactivity (Figure 4A). At 5 days following wounding, in the buffer-treated control wounds, there is a notable absence of CRT in the migrating keratinocytes both emanating from the wound margins (not shown) and those migrating upward from the hair follicles and sweat ducts (Figure 4B, arrow-

heads); these are the keratinocytes responsible for the formation of the epithelial islands within a partial thickness skin injury. In areas of mature stratified epidermis, CRT immunoreactivity is moderate, and still less than in unwounded epidermis (not shown). In the granulation tissue, there is a marked increase in the number of cells showing strong immunoreactivity for CRT (Figure 4B). Morphologically, these cells appear to be mainly fibroblasts and other connective tissue cells including immune cells. At 10 days after wounding, except the basal cells (arrows) and migrating epithelium (arrowheads), the keratinocytes composing the hypertrophic epidermis, particularly in the more differentiated stratum spinosum layer, still express ample amounts of CRT whereas the expression of CRT by the cells of the neodermis has greatly waned (Figure 4C). In the steroid-impaired animals, at 7 days after wounding, the wounds appeared similar to the (normal) unimpaired wounds with respect to the distribution of CRT immunoreactivity in the epidermis (Figure 4F). The intensity and number of cells expressing CRT in the neodermis appeared to be at inter-

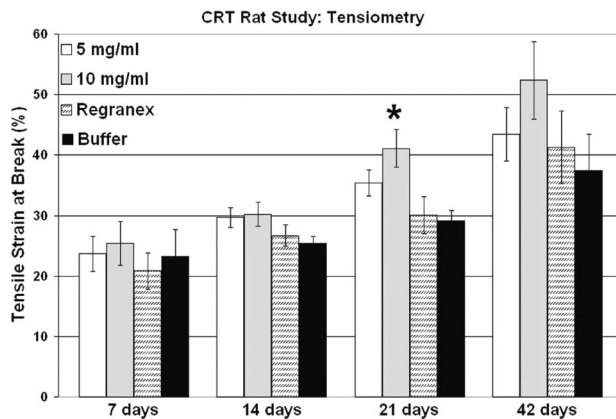


**Figure 3.** The effect of calcitriol on wound tensile strength (breaking strength) in a rat incisional model at 7, 14, 21, and 42 days after wounding. Four incisional wounds were created on each rat, which were approximated with clips, and four different treatments were applied: 5.0 and 10 mg/ml CRT, buffer, and PDGF-BB;  $n = 10$  rats/treatment/time point. After the 7, 14, 21, and 42 days, wound breaking strength was measured with a tensiometer. After 21 days treatment with 10 mg/ml CRT induces greater wound breaking strength than either buffer ( $*P \leq 0.001$ ) or PDGF-BB ( $**P \leq 0.027$ ), and CRT-treated (5.0 mg/ml) wounds are greater than buffer alone ( $P \leq 0.019$ ) but not greater than wounds treated with PDGF-BB.

mediate levels (Figure 4F) between the 10-day postinjury wounds of the normal untreated nonimpaired pigs (Figure 4C), which was low, and the higher immunoreactivity observed in the PDGF-BB-treated wounds (Figure 4, D and E). Interestingly, cells of the dermis of the Regranex-treated wounds expressed higher amounts of CRT (Figure 4, D and E) than the buffer control wounds at both 5 and 10 days after injury (Figure 4B and C). The very apparent up-regulation of CRT in the healing dermis of the PDGF-BB-treated wounds suggests that CRT is increased in wounds in which wound healing is stimulated.

### Topical Application of Calcitriol to Wounds Induces the Expression of TGF- $\beta$ 3

TGF- $\beta$  isoforms are important regulators of many aspects of wound healing, including induction of extracellular matrix proteins, such as collagens and fibronectin, and chemoattraction of cells into the wound.<sup>47-50</sup> Moreover, TGF- $\beta$  isoforms are differentially up-regulated, temporally and spatially, during wound repair, including in a porcine model of repair<sup>49,50,51</sup> indicating specific biological effects of the individual isoforms. Consistent with the apparent enhanced dermal repair in the CRT-treated wounds (Figures 1 and 2), using these same antibodies,<sup>51</sup> we show that the specific expression of the TGF- $\beta$ 3 isoform (Figure 5B) but not TGF- $\beta$ 1 (Figure 5C) or TGF- $\beta$ 2 (Figure 5D) is strongly increased in the dermal cells of the CRT-treated wounds compared to the buffer-treated wounds Figure 5A, shown here at 5 days after wounding. PDGF-BB- and buffer-treated wounds show equal intensity of immunostaining at this time point. Whereas a dose-dependent increase in TGF- $\beta$ 3 immunoreactivity was observed in wounds at 10 days after wounding (not shown), the intensity of TGF- $\beta$ 3 immunoreactivity was diminished compared to the earlier 5-day postinjury wounds.

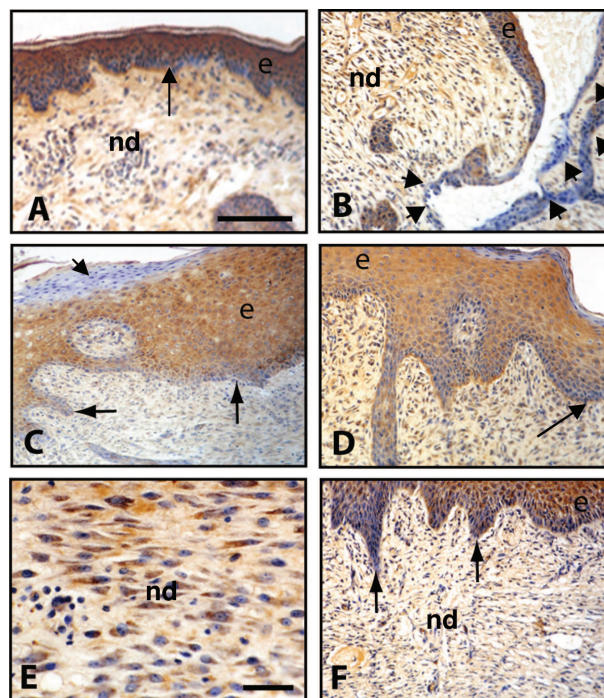


**Figure 4.** Immunostaining for endogenous calcitriol in buffer-treated and Regranex-treated porcine wounds evaluated at 5 and 10 days after injury. Unwounded skin (adjacent to a buffer-treated wound) (A); the wound at 5 days after wounding (B); 10 days after wounding (C-E); wounds from steroid-impaired pigs 7 days after wounding (F); buffer-treated wounds (B, C, F); PDGF-BB-treated wounds (D, E). Unwounded skin shows intense immunoreactivity within all of the differentiated layers of the epidermis in sharp contrast to the proliferative basal and suprabasal keratinocyte layer, which shows slight to no immunoreactivity (A). This lack of immunoreactivity in the basal layer of the epidermis is also observed at 5 days (B) and 10 days (C, D) after injury in normal wound healing (B) and after 7 days of healing in the steroid-impaired pig wounds (arrows) (F). There is a lack of CRT expression in the migrating epithelial tongue advancing over the wound (C, arrowhead). Similarly, the keratinocytes migrating upward from the hair follicles and sweat ducts to form epithelial islands lack CRT immunoreactivity (B, arrowheads). In contrast, CRT immunoreactivity is notable in the stratified hypertrophic differentiated epidermis of the buffer-treated wounds (C) and in the neodermis of the PDGF-BB-treated (D, E) wounds shown here at 10 days after injury and in the neodermis of the PDGF-BB and at 7 days postinjury in the steroid-challenged wounds (F). Multiple dermal cells are strongly immunoreactive for CRT protein in the buffer-treated wounds at 5 days after wounding (B). By 10 days, dermal immunoreactivity has decreased in the buffer-treated wounds (C) in contrast to the PDGF-BB-treated wounds (D, E). e, epidermis; nd, neodermis; arrows indicate basal epidermal cells with weak immunoreactivity for calcitriol; arrowheads indicate migrating epithelium. Brown represents DAB positive immunoreactivity and the blue color is the hematoxylin counterstain. Scale bars: A-D, F = 500  $\mu$ m; E = 30  $\mu$ m.

### Topical Application of Calcitriol to Wounds Stimulates Cellular Proliferation of Basal Keratinocytes and Presumptive Fibroblasts of the Dermis

Cellular proliferation of keratinocytes to resurface the denuded wound and of fibroblasts to increase the number of cells engaged in matrix production is critical to the wound repair process. To assess the effect of CRT on the cellular proliferation in porcine wounds treated with CRT *in vivo*, tissues from excised wounds were subjected to immunohistochemical staining using a standard proliferative cell marker, kinetochore nuclear protein 67 (Ki-67). After wounding, keratinocytes first migrate over the wound and do not show evidence of proliferation in the regenerative suprabasal and basal layers until

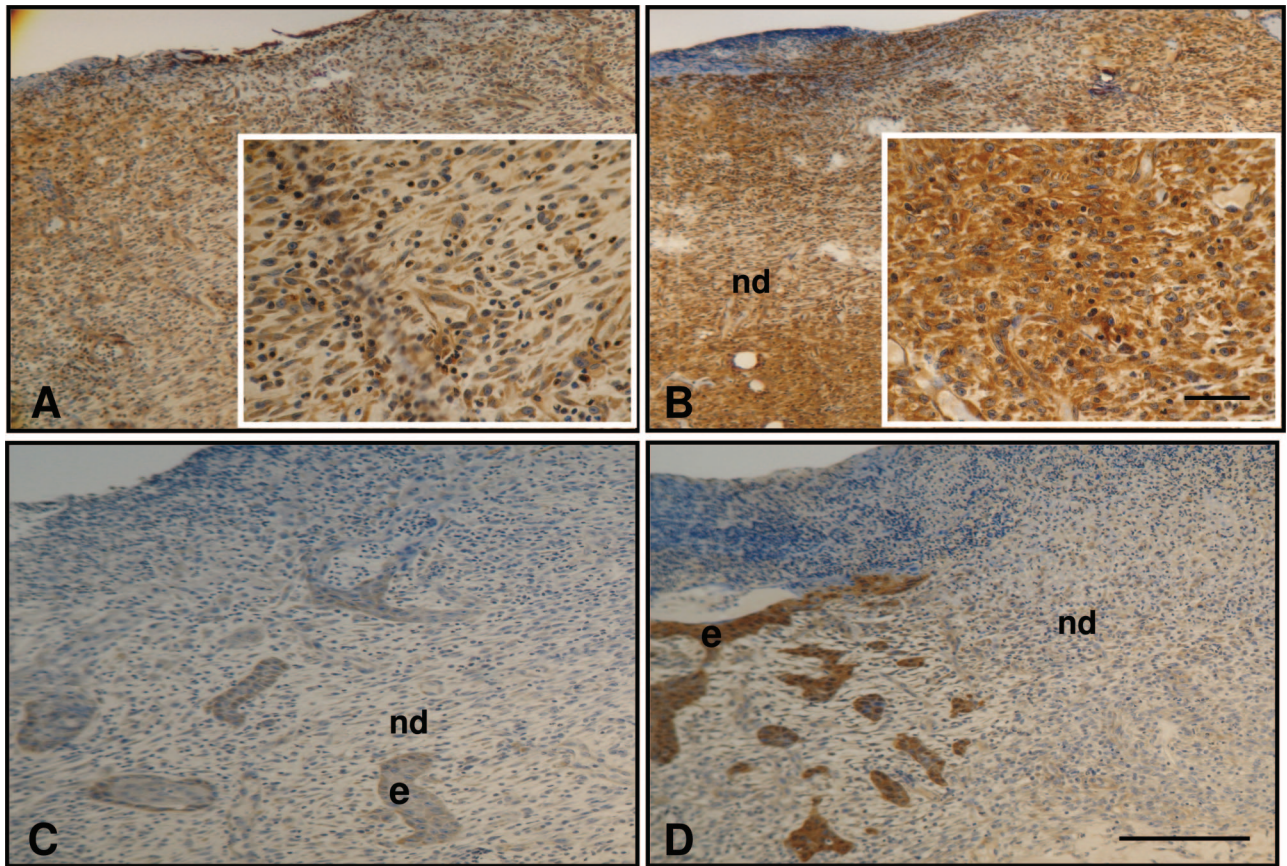


**Figure 5.** Immunostaining for TGF- $\beta$  isoforms in calreticulin-treated normal porcine wounds. Immunoreactivity for TGF- $\beta$ 3 (**A, B**), TGF- $\beta$ 1 (**C**), and TGF- $\beta$ 2 (**D**) after 5 days of healing. Buffer-treated wound (**A**); CRT-treated wounds (**B–D**). A marked intensity of immunoreactivity for TGF- $\beta$ 3 was observed in the granulation tissue of the 5.0 mg/ml CRT-treated wounds at 5 days after injury (**B**) compared to the buffer-treated wounds (**A**); the magnified insets show the intense cellular TGF- $\beta$ 3 immunostaining in the CRT-treated wounds. The newly forming epidermis was moderately immunostained for TGF- $\beta$ 3 (not shown). In contrast, neither TGF- $\beta$ 1 (**C**) nor TGF- $\beta$ 2 expression (**D**) was induced by 5.0 mg/ml CRT in the neodermis. Whereas TGF- $\beta$ 2 immunoreactivity was shown in the newly forming epidermis (**D**), no further induction by CRT was observed. Brown represents DAB positive immunoreactivity and the blue color is the hematoxylin counterstain. Scale bars: **A–D** = 300  $\mu$ m; **insets** = 30  $\mu$ m. e, epidermis; nd, neodermis.

resurfacing is complete. Wounds from the normal pig treated with CRT at 5 days after injury show a dose-dependent response in epidermal resurfacing and a corresponding intense Ki-67 immunoreactivity in basal and suprabasal keratinocytes (Figure 6, A and B, arrows). In contrast, there were markedly fewer immunoreactive basal keratinocytes in the buffer-treated (Figure 6C) and Regranex-treated (Figure 6D) wounds that show variable and barely (delayed) resurfaced wounds. Marked immunoreactivity is observed in dermal cells of the CRT-treated and PDGF-BB-treated wounds Figure 6B and D. With higher magnification, these dermal cells appear to be largely fibroblasts. In the more mature wounds at 10 days after wounding, proliferation in the neodermis subsided, being replaced by matrix production (not shown).

Similar to the results obtained with the normal pigs, in the steroid-challenged pigs, CRT treatment induced a strong dose-dependent effect on the proliferation of basal and suprabasal keratinocytes (arrows) in the 7-day postinjury re-epithelialized wounds and in dermal cells (presumptive fibroblasts; Figure 6, E–G). As these wounds had re-epithelialized, the buffer-treated and PDGF-BB-treated wounds show equal numbers of proliferating cells in the basal layer of the epidermis (Figure 6, H and I), albeit notably less than the CRT-treated wounds (Figure 6, E–G). The intensity of

immunoreactivity in the dermal cells was similar in the Regranex- (Figure 6I) and 5 mg/ml CRT-treated wounds (Figure 6E). Therefore, topical application of CRT to porcine wounds has a marked effect on cellular proliferation of both the epidermal and dermal aspects of repair in both normal and steroid-impaired wound healing. The specificity of CRT on cellular proliferation in the epidermis and dermis during wound healing is corroborated by the dose-response effect obtained and the *in vitro* studies described below.

#### *Calreticulin Stimulates Cellular Proliferation of Human Keratinocytes, Fibroblasts, and Microvascular Endothelial Cells*

The intense immunostaining for Ki-67 antigen in basal keratinocytes and dermal cells suggested that CRT might directly stimulate cellular proliferation, an important characteristic for both generating a stratified epidermal layer and for populating the dermis with ample cells to produce cytokines and extracellular matrix proteins. Therefore, we tested the effect of CRT on human primary keratinocytes and human dermal fibroblasts *in vitro*. Increasing doses of CRT (0–200 pg/ml) were added to synchronized sub-

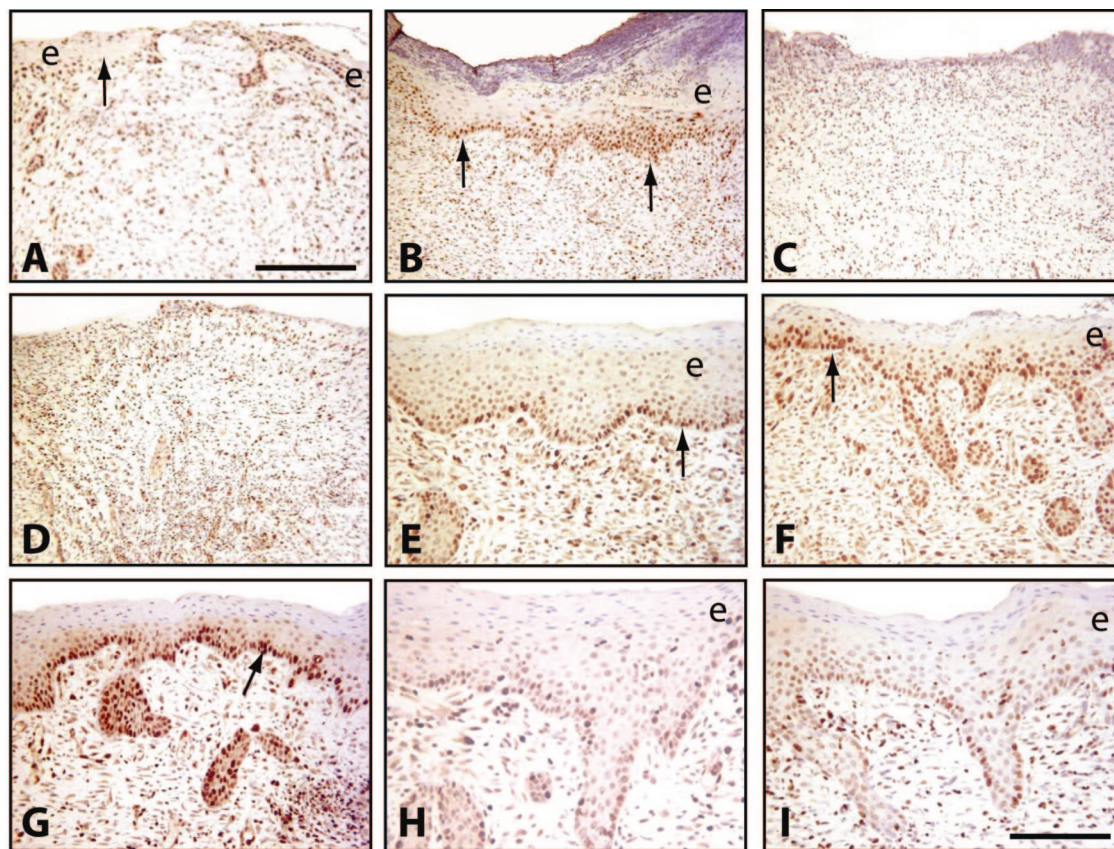


**Figure 6.** Immunostaining for proliferating cells (Ki-67) in calreticulin-treated normal and steroid impaired porcine wounds. Wounds from normal pigs at 5 days after healing (**A–D**); wounds from steroid-impaired pigs at 7 days after healing (**E–I**). Treatments: 1.0 mg/ml CRT (**A**), 5.0 mg/ml (**B, E**), 10 mg/ml CRT (**F**), 50 mg/ml CRT (**G**), buffer (**C, H**), and PDGF-BB (**D, I**). CRT treatment induced a dose-dependent increase in the number of proliferating basal and suprabasal keratinocytes (arrows) (epidermal replenishment compartment) in the immature epidermis of the CRT-treated normal wounds (**A, B**) compared to the buffer-treated (**C**) and PDGF-BB-treated (**D**) wounds, showing no epidermal resurfacing. In the wounds of the steroid-challenged pigs, CRT at 5.0 mg/ml (**E**), 10 mg/ml (**F**), and 50 mg/ml (**G**) is shown to induce a dose-dependent increase in proliferating keratinocytes in the basal layers of the epidermis compared to buffer-treated (**H**) and PDGF-BB-treated (**I**) wounds, which show relatively fewer Ki-67 positive nuclei in the hypertrophic epidermis. There were numerous proliferating cells (presumptive fibroblasts) in the neodermis of both the CRT- and PDGF-BB-treated normal (**A, B, D**) and steroid-impaired (**E–G, I**) pigs compared to the buffer controls (**C, H**). The dose-dependent response of the CRT-treated wounds was also evident in the neodermis of the normal wounds (**A, B**). Arrows indicate Ki-67 positive proliferating basal keratinocytes. Brown represents DAB positive immunoreactivity and the blue color is the hematoxylin counterstain. Scale bars: **A–D** = 445  $\mu$ m; **E–I** = 225  $\mu$ m.

confluent human primary keratinocytes. After 72 hours, a dose-dependent increase in cellular proliferation was obtained, with a peak response of 2.2-fold over untreated controls, with 100 pg/ml CRT (Figure 7A;  $n = 5$ ) that returned to normal control levels at 200 pg/ml. A similar peak response was obtained in unsynchronized cultures of keratinocytes that were incubated with CRT in basal medium for 48 hours ( $n = 2$ ). The response is compared to human EGF (10 ng/ml) as a positive control which gave a smaller peak response of 1.3-fold in both assays.

CRT (0–200 ng/ml) similarly stimulated synchronized subconfluent human primary dermal fibroblasts in a dose-dependent manner after 72 hours of incubation, yielding a peak response, with 100 ng/ml CRT that was 2.4-fold higher than the untreated controls (Figure 7B;  $n = 7$ ). This response was similar to FGF (5.0 ng/ml) as a positive control. It is notable that keratinocytes were more sensitive to CRT, with a peak response 1000-fold less than the fibroblasts (100 pg/ml versus 100 ng/ml). In one experiment, we tested the effect of recombinant human CRT on fibroblast proliferation and obtained the identical specific activity as the recombinant rabbit CRT used for all of the *in vivo* and *in vitro* experiments (Figure 7C).

CRT dose-dependently stimulated proliferation of human microvascular endothelial cells after 24 hours of incubation of the cells with 0 to 100 pg/ml CRT. Although the response obtained was small, the endothelial cells were highly sensitive to CRT with a consistent peak response of 30% increase in proliferation over the control with 1.0 to 25 pg/ml CRT (Figure 7D;  $n = 5$ ), which was equal to 10 ng/ml VEGF as the positive control (not shown). In contrast, *in vivo*, neither CRT nor PDGF-BB appeared to induce an increase in microvascular density in either the normal or steroid-impaired porcine wounds as assessed using an antibody to factor VIII (anti-CD31) as a marker of endothelial cells (not shown). Possibly the magnitude of the *in vivo* effect was too low to be statistically significant in the small number of wounds in this study.

#### *Calreticulin Induces Migration of Keratinocytes and Fibroblasts*

In the cellular context, re-epithelialization and dermal remodeling *in vivo* are dependent on, and thus largely reflect, both the biological processes of cellular proliferation and migration. A standard scratch plate assay to simulate

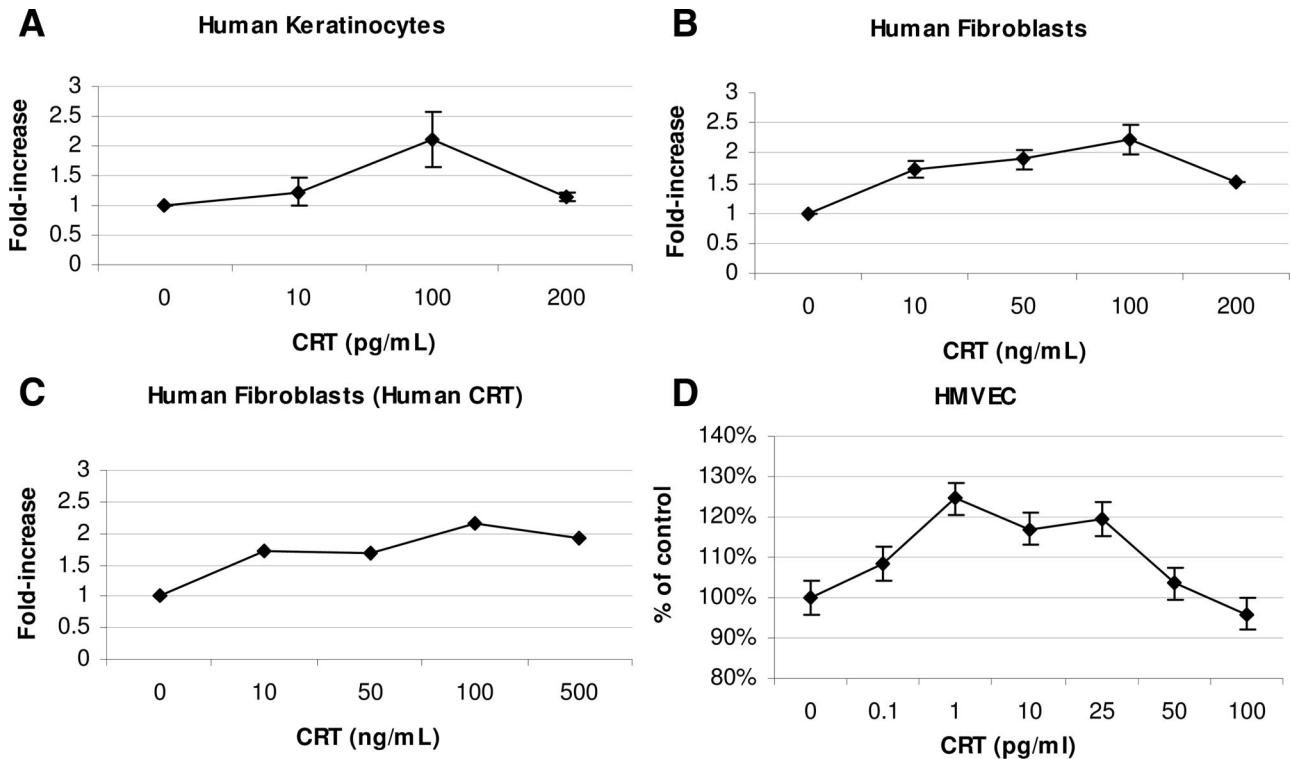


**Figure 7.** Calreticulin induces cellular proliferation of primary human keratinocytes, fibroblasts, and microvascular endothelial cells. **A:** Keratinocytes. Increasing concentrations of CRT (0–200 pg/ml) were added to subconfluent synchronized primary keratinocytes in KBM on 96-well plate for 72 hours, and the MTS proliferation assay (CellTiter96) was performed in triplicate. EGF (10 ng/ml) was used as a positive control (not shown). The data are expressed as fold increase  $\pm$  SEM compared to cells treated with KBM alone. Maximal stimulation of 2.2-fold was achieved with 100 pg/ml CRT and 1.3-fold with EGF ( $n = 5$ ). **B:** Fibroblasts. Increasing concentrations of CRT (0–200 ng/ml) were added to human primary subconfluent synchronized fibroblasts in MEM containing 0.5% serum on a 96-well plate for 72 hours, and the MTS assay performed in triplicate; FGF at 5.0 mg/ml was added as a positive control (not shown). The data are expressed as fold increase  $\pm$  SEM over control in MEM. An equal peak response of 2.4-fold was obtained with both 100 ng/ml CRT and the FGF positive control ( $n = 7$ ). **C:** A similar response was obtained using human recombinant CRT ( $n = 1$ ). **D:** Human primary microvascular endothelial cells. Increasing concentrations of CRT (0–100 pg/ml) in EGM containing 0.5% serum were added to subconfluent synchronized human primary microvascular endothelial cells on a 96-well plate in triplicate for 24 hours and the MTS assay performed. The data are expressed as fold increase over control cells incubated with 0.5% serum. VEGF at 10 ng/ml served as a positive control (data not shown). A 30% increase in proliferation over the control was obtained with both 1 to 25 pg/ml CRT and VEGF ( $n = 5$ ).

wound healing *in vitro* was used to assess the effect of increasing concentrations of CRT on migration/motility on the human primary keratinocytes and fibroblasts.<sup>52,53</sup> The graph (Figure 8A) shows that CRT (0–100 pg/ml) induces a dose-dependent increase in the number of keratinocytes (represented as percent wound closure) covering the wound at 48 hours after treatment. A peak response of  $16.8\% \pm 1.53$  wound closure with 10 pg/ml CRT was obtained compared to the EGF (10 ng/ml) positive control yielding 11.6% closure, but statistically significantly more than the media control, at 2% closure ( $P \leq 0.003$ ;  $n = 5$ ). Similar results were obtained in experiments performed in the presence of 1 to 5  $\mu\text{g/ml}$  mitomycin C in the migration assay (data not shown) and thus, cellular proliferation did not appear to be a component of the migratory response to CRT. Using a thin-membrane ChemoTx chamber system, CRT (1–750 pg/ml) induces a concentration-dependent migration of keratinocytes through the membrane with an optimal dose of 10 pg/ml, which represents an 18.43-fold increase over the media control (Figure 8, B and C) and a 2.5-fold increase over EGF used as a positive control. The dose-dependent response to CRT is clearly represented by the DAPI-stained nuclei of the keratinocytes on the bottom side of the membrane (Figure 8C) represented by the graph (Figure 8B,  $n = 5$ ). It is notable that the identical peak

response was obtained with both the scratch plate and directed migration assays using keratinocytes prelabeled with the fluoroprobe, calcein, or nuclei stained with DAPI following the assay (Figure 8, B and C).

Similarly, CRT induced a dose-dependent increase in migration of human fibroblasts in the scratch plate assay, with a maximal response of  $62\% \pm 5.3$  closure of the wound at 24 hours with 1 ng/ml CRT. The CRT-induced response was greater than both the positive (5% FBS) and negative (MEM) controls ( $P \leq 0.002$ ), which showed wound area closure by 58% and 24%, respectively (Figure 9A;  $n = 10$ ). A representative dose-response study is illustrated by the photomicrographs of the scratch plate assay in Figure 9C. The affect of CRT on cellular migration of fibroblasts was unaffected by the addition of 8.0  $\mu\text{mol/L}$  mitomycin C. Using the human fibroblasts in the thin-membrane ChemoTx chamber system, either prelabeled with calcein or stained at the completion of the assay with DAPI, CRT (1.0–100 ng/ml) induced directed migration of these cells in a concentration-dependent manner with a peak response at 10 ng/ml as shown by the graph in Figure 9B. Counting the cells/high power field, CRT induced a four-fold induction of migration compared to the negative media control with a similar response elicited by the FGF positive control at 3.5-fold ( $n = 3$ ).

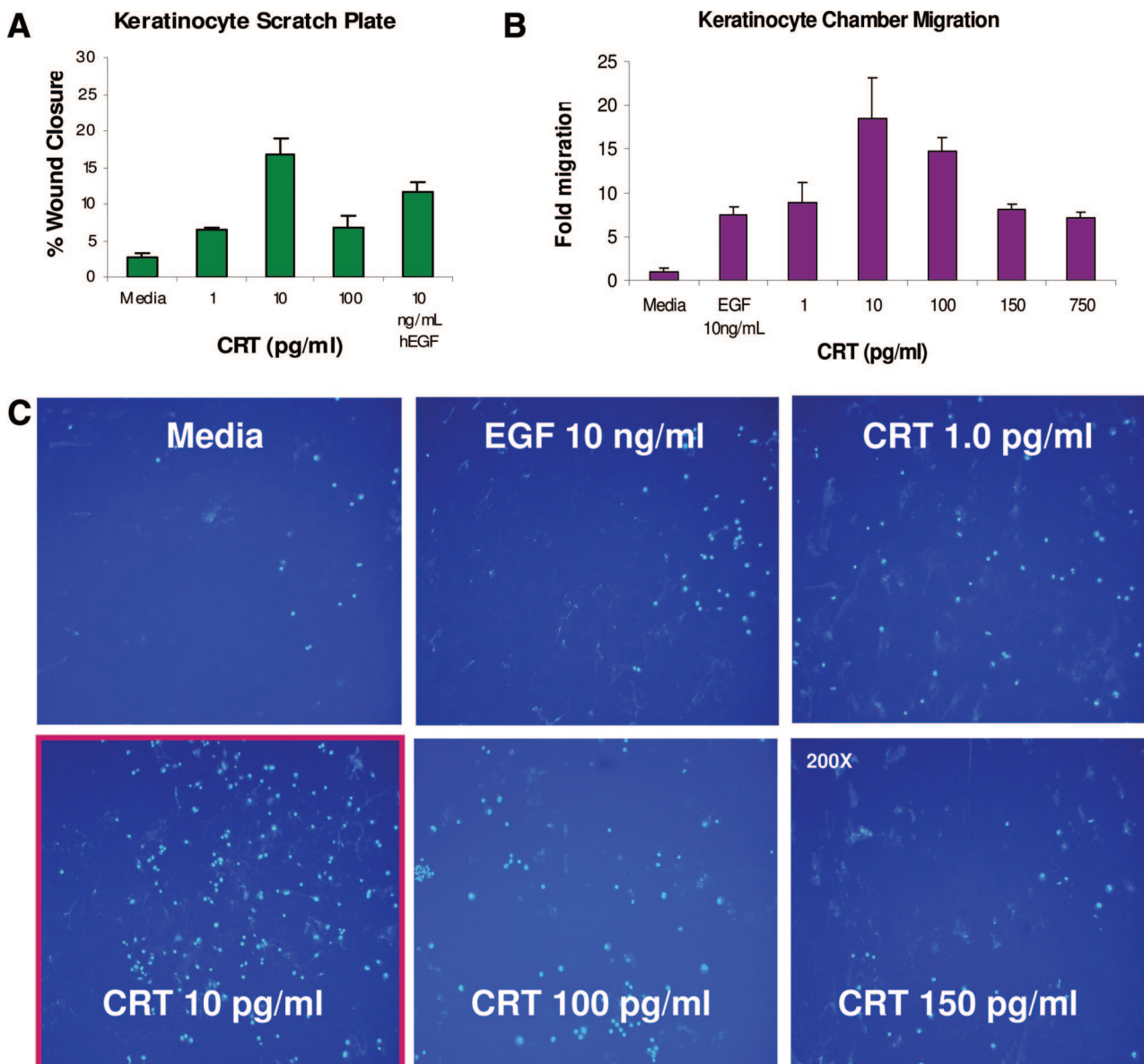


**Figure 8.** Calreticulin induces cellular migration of human primary keratinocytes in the scratch plate assay as an *in vitro* model of wound healing and elicits concentration-dependent migration using a chamber assay. **A:** Scratch plate assay/graph. Primary human keratinocytes were seeded on 24-well tissue culture plates, grown to 70 to 80% confluence in keratinocyte growth medium, and switched to KBM for 18 hours. The plate was scratched with a plastic pipette tip, and increasing concentrations of CRT (0–100 ng/ml) added to the cells. After 48 hours, migration over the wound was measured as described in Materials and Methods. As shown by the graph, CRT induces a dose-dependent increase in the number of cells that migrated into the wound with a peak response of 16.8% closure of the wound with CRT at 10 pg/ml ( $P \leq 0.003$  compared with medium alone;  $n = 5$ ). EGF (10 ng/ml) as a positive control induced 11.6% closure. **B:** Chamber migration assay/graph. Keratinocytes were washed, treated with trypsin, centrifuged, and applied to a membrane with an 8.0- $\mu\text{m}$  pore size at a concentration of  $2.5 \times 10^4$ /well (96-well plate; ChemoTx migration system, Neuroprobe) in KBM as described in Materials and Methods. The bottom migration wells contained increasing dilutions of CRT (1–750 pg/ml) in KBM. After 4 hours at 37°C, the membranes were removed from the wells, and the cells on the bottom of the membranes fixed with 4% paraformaldehyde for 5 minutes and then applied to coverslips that were sealed and stained with VECTASHIELD DAPI. The membranes were photographed at 200 $\times$  and the number of cells counted in at least 6 high-power fields. Treatments were in triplicate and EGF (10 ng/ml) served as positive control. The graph, shown as fold migration over the media control, shows that CRT induces a concentration-dependent directed migration of keratinocytes with peak response at 10 pg/ml (identical to the scratch plate assay) ( $n = 3$ ). The data show an 18.4-fold and 2.5-fold increase over the media and EGF control, respectively. Error bars represent SEM. **C:** Photomicrograph of keratinocyte migration in one representative thin-membrane chamber migration assay demonstrating the concentration-dependent effect of CRT peaking at 10 pg/ml as illustrated by the red box around the panel. It is notable that keratinocytes are more sensitive to CRT than the positive EGF control.

As with the proliferative response, keratinocytes demonstrate greater sensitivity to CRT than the fibroblasts as a 10,000 times lower dose was required for the maximal migratory response (10 pg/ml versus 1 ng/ml; compare Figures 8A and 9A) in the scratch plate assays. In addition, in this assay, it is shown that the migratory response was of a higher magnitude with the fibroblasts than the keratinocytes

(80% versus 15%). This is likely related to the greater cell density at the time of performing the scratch on the plate as it is notable that the intensity of the response was not so disparate between these two cell types in the chamber migration assay. The proliferation and migration responses obtained *in vitro* provide mechanistic support for the histological effects shown in the CRT-treated wounds.

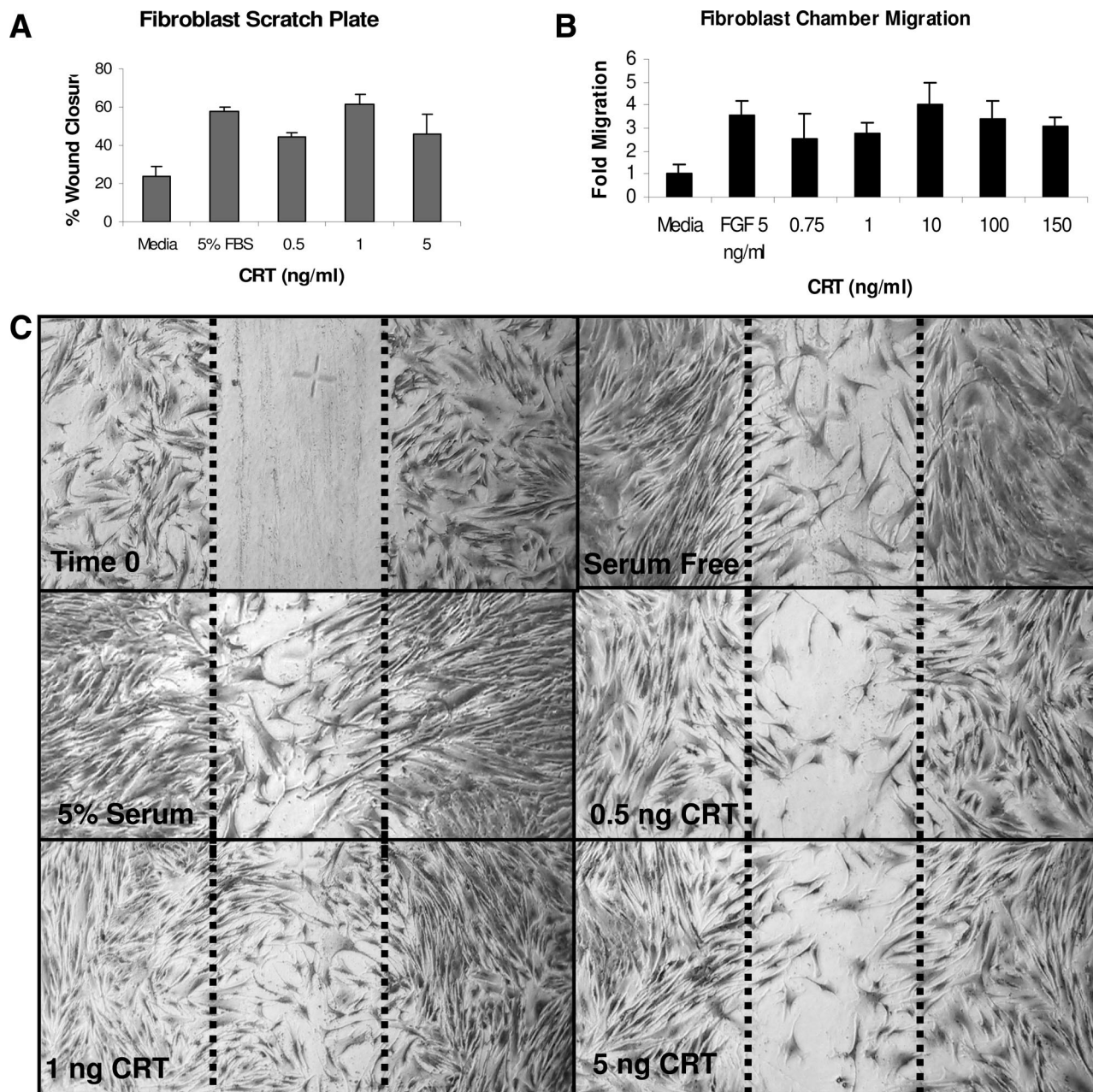


**Figure 9.** Calreticulin induces cellular migration of human primary fibroblasts in the scratch plate assay as an *in vitro* model of wound healing and elicits a concentration-dependent migration using a chamber assay. **A:** Scratch plate assay. Primary human dermal fibroblasts were plated in 24-well plates grown to 70 to 80% confluence in MEM containing 10% FBS for 24 hours, wounded, and increasing concentrations of CRT (0–10 ng/ml) in MEM added to the cells. After 24 hours, CRT was shown to induce a dose-dependent increase in the number of cells that migrated over the wound with a peak response of  $62\% \pm 5.3$  closure with 1.0 ng/ml CRT compared to MEM alone at 24% ( $P \leq 0.002$ ;  $n = 10$ ). FBS, 5.0%, as a positive control induced 58% wound closure. **B:** Chamber migration assay. Fibroblasts were washed, treated with trypsin, centrifuged, and applied to a membrane with an 8.0- $\mu\text{m}$  pore size at a concentration of  $5.0 \times 10^4$ /well (96-well plate; ChemoTx Neuroprobe) in serum-free MEM as described in Materials and Methods. The bottom migration wells contained increasing dilutions of CRT (1.0–150 ng/ml) in MEM. After 4 hours at 37°C, the membranes were removed from the wells, and the cells were fixed and then stained with VECTASHIELD DAPI, and the number of cell/high power field counted as described in Figure 8B. Treatments were in triplicate and FGF (5.0 ng/ml) served as positive control. The graph shows that CRT at 10 ng/ml induces a concentration-dependent directed migration of fibroblasts with a four-fold peak over the media control ( $n = 3$ ), which was similar to the FGF positive control at 3.5-fold. Error bars represent SEM. **C:** Photomicrographs of one representative scratch plate assay of human dermal fibroblasts (stained with Coomassie blue as described in Materials and Methods) at the end of the 24-hour incubation time shows that CRT induces dose-dependent migration with a maximal response at 1.0 ng/ml.

### Calreticulin Induces Influx of Monocytes/Macrophages into the Wounds

CRT has the auspicious function of being the obligate mediator of apoptotic cell clearance by both “professional” and “nonprofessional” phagocytes.<sup>26</sup> Since ac-

cumulation of dead cells and tissue are important retardants to the wound healing process, such a functional role for CRT in wound healing would be unequivocally significant. Therefore, we analyzed the effect of CRT on the influx of monocytes/macrophages, one of the major professional phagocytic cell types,

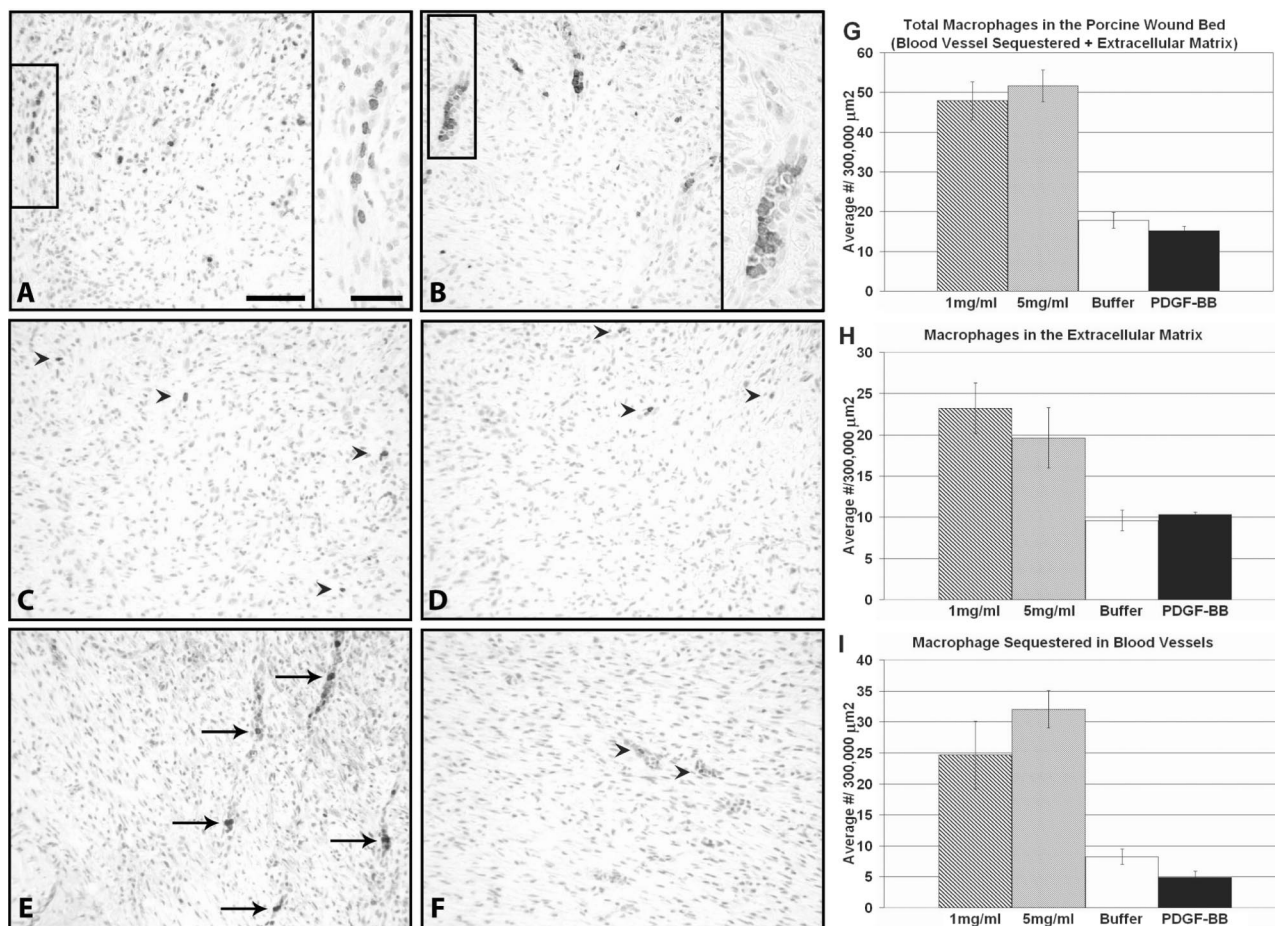


**Figure 10.** Calreticulin induces macrophage influx into wounds in normal and steroid-impaired pigs shown at 5 days after injury. **A:** Immunohistochemistry for monocytes and macrophages using MAC-387 antibody on wound tissue at 5 days of healing in the normal (**A–D**) and steroid-impaired pig at 7 days of healing (**E, F**). Treatments: 1.0 mg/ml CRT (**A**); 5.0 mg/ml CRT (**B, E**); buffer (**C, F**); PDGF-BB (**D**). Macrophages are notable within the vasculature and ECM of the neodermis following treatment with either 1.0 mg/ml (**a**) and 5.0 mg/ml (**b**) CRT. The **inset** highlights the distribution of macrophages in the capillaries. In contrast, few macrophages are shown in the buffer-treated (**C**) and PDGF-BB-treated (**D**) wounds. CRT at 5.0 mg/ml increases macrophage influx into the wounds of steroid-challenged pigs, which show many macrophages sequestered within the capillaries of the neodermis (**E**). A small number of macrophages was observed in the buffer-treated wounds of the steroid-challenged pigs (**F**). Scale bars: **A–F** = 50  $\mu\text{m}$ ; **insets** = 30  $\mu\text{m}$ . **B–D:** Quantitative morphometric analysis of MAC-387 positive macrophages in normal porcine wounds harvested after 5 days of healing. **G:** Graphs of the total number of monocytes/macrophages (in 300,000  $\mu\text{m}^2$ ) in the porcine wound bed (both sequestered within the capillary network and extravascular). Treatment of the porcine wounds with either 1.0 or 5.0 mg/ml CRT induced a more than threefold increase in the number of macrophages in the wound granulation tissue compared to the buffer or PDGF-BB control groups ( $P \leq 0.008$ ). **H:** Graph of macrophages within the extracellular matrix excluding monocytes/macrophages within the vascular networks of the granulation tissue. The numbers of macrophages in this compartment are approximately twofold more in the CRT-treated wounds than the buffer or PDGF-BB treatments ( $P < 0.009$ ). **I:** Macrophages/monocytes that remained sequestered within the vascular network of capillary tissue is sixfold higher than buffer ( $P < 0.001$ ;  $n = 6$  wounds/treatment).

into the porcine wounds. Immunohistochemical staining for macrophages revealed that wounds treated with both 1.0 and 5.0 mg/ml CRT contained numerous macrophages at 5 days after wounding, when macrophage influx is typically at maximal levels (Figure 10A and B). Quantitation of the number of macrophages in the tissues revealed an average of 48 and 51 cells/300,000  $\mu\text{m}^2$  high power field following treatment with 1.0 and 5.0 mg/ml CRT, respectively. In contrast, an average of 19 and 15 macrophages/high power field was obtained in the buffer and PDGF-BB-treated wounds (compare Figure 10A, and B, to C and D; 10G). Thus, there was approximately three times the number of macrophages/high power field in the granulation tissue of the CRT-treated compared to the buffer or PDGF-BB-treated wounds (Figure 10G;  $P \leq 0.008$ ). Following examination of the tissues from the steroid-challenged pigs at 7 days

after wounding, a similar increase in the influx of macrophages into the wounds was observed (Figure 10A, E and F). After 10 days of repair in the normal wound model, the prevalence of macrophages was markedly diminished in all groups (data not shown), indicating that CRT does not prolong or sustain the influx of macrophages past the normal resolution of the inflammatory phase of repair.

Interestingly, many of the immunoreactive monocytes/macrophage were sequestered within the lumen of the capillary network of the neodermis in the healing wounds from both the normal (Figure 10A, and B and enlarged insets; Figure 10D), and steroid-challenged pigs (Figure 10A, e and f). This prompted the counting of macrophages that were localized within the extracellular matrix of the neodermis (not inside capillaries) (Figure 10H) and subtracting this amount from the total

(Figure 10G) thus, providing the number of macrophages sequestered within the dermal capillary network (Figure 10I). A statistically significant effect of both 1 and 5 mg/ml CRT in recruiting macrophages within the vascular compartment ( $P \leq 0.001$ ) and extracellular matrix of the neodermis ( $P \leq 0.09$ ) was obtained (Figures 10H and I) compared to the PDGF-BB- and buffer-treated wounds.

### *Calreticulin Induces Concentration-Dependent Directed Migration of Human Monocytes and Macrophages*

Since CRT treatment of both the normal and steroid-impaired wounds appeared to have a profound affect on recruiting monocytes/macrophages into the wound bed, we performed ChemoTx chamber migration assays using both human THP-1 monocytes and their phorbol 12-myristate 13-acetate-induced differentiated macrophage counterparts either prelabeled with calcein or stained at termination of the migration assay with DAPI. As shown by the graph in Figure 11A, monocytes that were prelabeled with the calcein fluorescent probe, before performing the chamber migration assay, migrate in a concentration-dependent directed manner in response to CRT (0.5–50 ng/ml with a peak response of 1.0 ng/ml, which is equal to the highest dose of fMLP (100 nmol/L) positive control ( $n = 3$ ). As illustrated by the DAPI-stained macrophages that have migrated within the membranes to 0.5 to 50 ng/ml of CRT, (Figure 11C), CRT induces a concentration-dependent directed migration of macrophages with a peak response between 1.0 and 5.0 ng/ml (Figure 11B;  $n = 8$ ). CRT at 5.0 ng/ml stimulated a seven-fold increase in the number of cells that migrated through the membrane compared to the media control and a two-fold increase over the positive controls of fMLP and VEGF, which were equal. Similarly, these *in vitro* results strongly support our findings *in vivo* and show an important role for CRT in the recruitment of monocytes from the circulation into the wound bed for the critical functions of cytokine production and wound debridement.

### *Discussion*

Our studies show that the ER chaperone protein CRT demonstrates widespread multicellular effects on critical aspects of the wound healing process. Interestingly, similar to CRT, a number of major stress-induced ER chaperone proteins containing KDEL ER retention sequences demonstrate extracellular functions.<sup>54–56</sup> For example, as we have found for CRT, exogenous application of either hsp-90 or hsp-70 accelerated murine wound repair<sup>56,57</sup> and hsp-47 is up-regulated during the wound repair process.<sup>58</sup> In addition, diabetic mice fail to up-regulate hsp-70 as a consequence of delayed repair.<sup>59</sup> Therefore, stress-induced proteins such as CRT appear to have separate intracellular and extracellular functions as physiological mediators of wound healing. Specifically, we envision that intracellular CRT is up-regulated during the

oxidative stress of a wound environment by exerting a positive influence in the production of protective proteins.<sup>2</sup> Since an exit mechanism for CRT into the extracellular compartment has been difficult to demonstrate, we propose that on injury and cell death, CRT is spewed into the microenvironment to function extracellularly by induction of cellular activities required for healing wounds, exemplified by our studies shown herein. In this context, the dynamic expression of CRT that we show during porcine wound healing might implicate an important physiological role for CRT in the wound healing process. The exogenous topical application and thus, greater saturation of CRT at the wound site might enhance these effects providing potential use of CRT as a therapeutic agent for enhancing wound repair. Conversely, it is possible that only extracellular CRT might exert wound healing effects.

Topical application of CRT affected the two most important processes required for proper and efficient healing, re-epithelialization of the wound and granulation tissue/neodermal formation. Re-epithelialization restores the surface barrier on the skin to prevent continuous loss of body fluids and proteins while impeding the entrance of harmful pathogens. The CRT-treated wounds resurfaced earlier than the buffer or PDGF-BB-treated wounds and exhibited a stratified, more mature epithelium with an intact stratum corneum. We anticipate that the beneficial biological effects of CRT on wound healing might be further enhanced if applied as PDGF-BB (Regranex) in a formulated gel, which both protects and prolongs the even release of proteins. Given that there were only six wounds/parameter (due to limited supply of CRT), the genetic heterogeneity among the pigs, that adolescent pigs exhibit a robust healing response with a small margin for improvement, and the suboptimal delivery of CRT in buffer, the trend represented by the graph might be more significant. Importantly, the marked proliferation in the basal and suprabasal keratinocytes coupled with the *in vitro* studies showing that CRT dose-dependently induces both migration and proliferation of keratinocytes at femtomolar concentrations supports the specific and strong effect of CRT on the epithelium. That PDGF-BB failed to show an effect on re-epithelialization is consistent with reports showing that the efficacy of this growth factor in enhancing wound healing is variable and model dependent and that it acts by stimulation of dermal wound healing events such as angiogenesis and granulation tissue formation and not through a direct mediation of re-epithelialization.<sup>60,61</sup>

Ample granulation tissue formation in the dermis is an important quality of wound repair. Fibroblasts are most responsible for producing the granulation tissue extracellular matrix (ECM), which both fills in the wound defect but first provides the scaffolding for the influx of cellular constituents such as keratinocytes, which use the matrix for migration to re-epithelialize the wound. CRT treatment of both the normal and steroid-impaired porcine wounds induced a dose-dependent increase in granulation tissue. The wounds were more cellular and the depth of granulation tissue exceeded the PDGF-BB-treated controls in the normal pigs at the earlier time point. However,

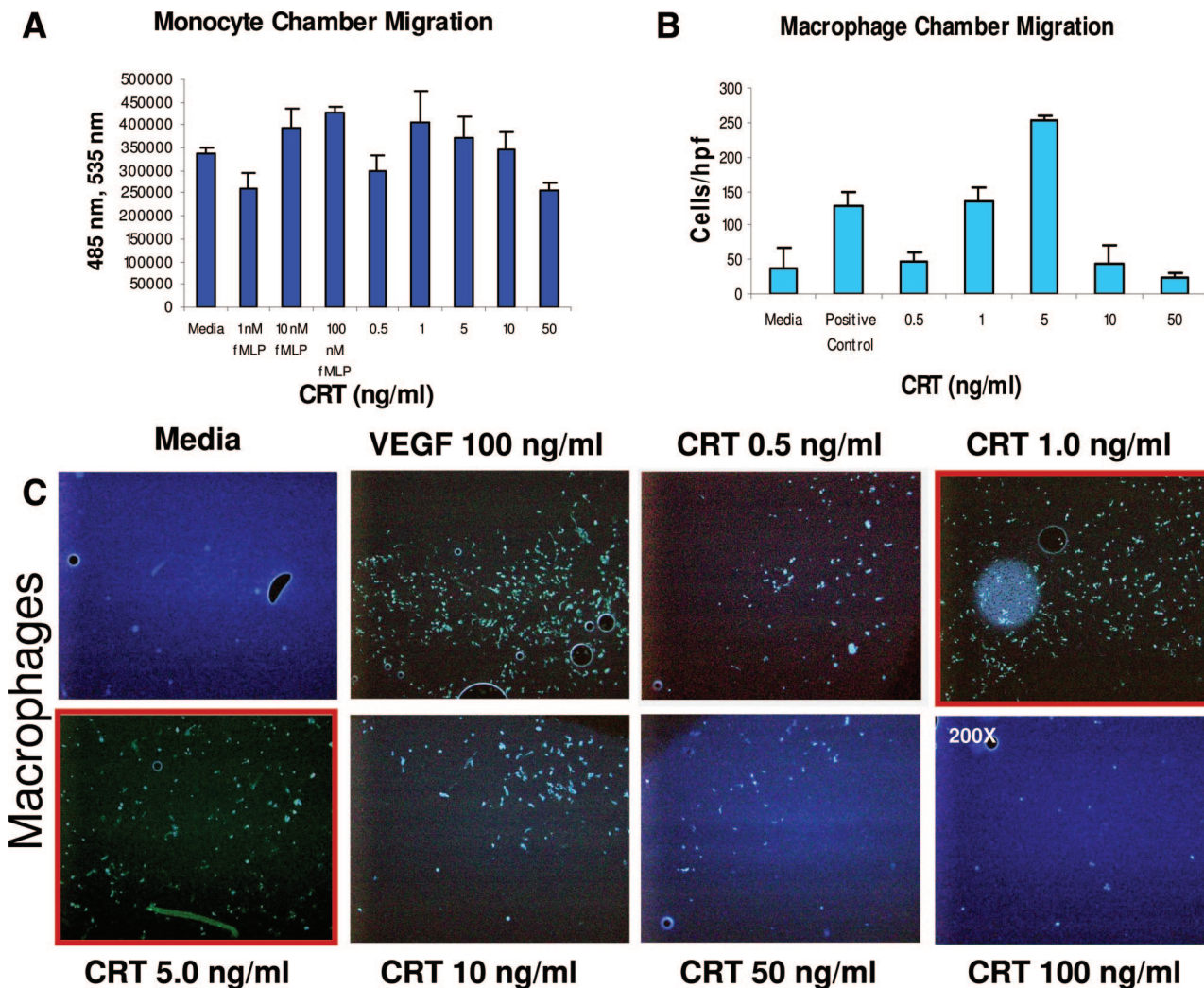


**Figure 11.** Calreticulin induces concentration-dependent migration of human monocytes and macrophages. **A:** Monocytes in a chamber migration assay. Human monocytes (THP-1 cell line) were incubated with 2.0  $\mu\text{mol/L}$  calcein for 40 minutes, washed in PBS, and added to a membrane with a 5.0- $\mu\text{m}$  pore size at a concentration of  $5.0 \times 10^4$ /well (96-well plate; ChemoTx Neuroprobe) as described in Materials and Methods. The bottom migration wells contained increasing concentrations of CRT (1.0–50 ng/ml) in RPMI 1640. After 1 hour at 37°C, the cells on top of the membrane were removed, and the plate was centrifuged to detach the cells lodged in the membrane into the bottom chamber. Fluorescence in the bottom wells was measured at excitation and emission wavelengths of 485 and 535 nm, respectively. Increasing concentrations of fMLP (1.0–100 nmol/L) served as a positive control and serum-free medium as a negative control. Treatments were performed in triplicate. As shown, CRT induces a concentration-dependent directed migration of the monocytes with a peak response at 1.0 ng/ml, which was equal to the fMLP control (100 nmol/L) in this one representative experiment ( $n = 3$ ). The error bars represent SEM for one experiment. **B:** Macrophages in a chamber migration assay. THP-1 monocytes were differentiated into macrophages by the addition of phorbol myristate acetate at 10 ng/ml for 48 hours. The cells were washed with PBS and then RPMI 1640 added to a membrane with a 5.0- $\mu\text{m}$  pore size at a concentration of  $2.5 \times 10^4$  cells/well (96-well plate; ChemoTx Neuroprobe) as described in Materials and Methods. Increasing concentrations of CRT (0.5–50 ng/ml) were in the bottom wells. After 2 hours of incubation, the membrane was removed from the chambers, the cells on the bottom of the membrane fixed and then stained with VECTASHIELD DAPI, and the number of cells per high power field counted as described in Figure 8B. Both fMLP (100 nmol/L) and VEGF (100 ng/ml) served as positive controls and media alone as a negative control. CRT at 5.0 ng/ml induces concentration dependent migration of macrophages with a peak response of sevenfold increase in the number of migratory cells compared to fMLP and VEGF, which both elicited a twofold response in different experiments ( $n = 8$ ). The error bars represent SEM. **C:** Photomicrograph of macrophage migration in one representative thin-membrane chamber migration assay demonstrating the concentration-dependent effect of CRT peaking at 1.0 to 5.0 ng/ml as illustrated by the red boxes around the panel, which is comparable to the VEGF positive control.

as observed in the healing epidermis, the CRT-treated wounds demonstrated a more mature compacted dermis than the buffer or PDGF-BB-treated wounds at the later time point, reflecting the accelerated rate of repair. Whereas both CRT and PDGF-BB-treated wounds appear to contain similar amounts of collagen, the breaking strength (tensile strength) data from the rat incisional wound model provide support that CRT enhances the quantity of collagen within the ECM. Surprisingly, these data reached statistical significance compared with PDGF-BB-treated wounds. The increase in collagen ac-

cumulation in the wound bed is likely related to the increase in numbers of morphologically appearing fibroblasts in the healing dermis and the marked increase in the expression of TGF- $\beta_3$ , known for its inductive effects on most matrix proteins.<sup>49,62,63</sup> Furthermore, the *in vitro* studies show a direct effect of CRT on human dermal fibroblast proliferation and migration thereby providing functional biological correlates to the enhanced dermal effects observed during wound repair.

The increased expression of CRT in dermal cells in response to cutaneous injury during wound healing and

greater induction of CRT by PDGF-BB purports a physiological role for this ER protein in promoting granulation tissue formation. It is notable that the effects of CRT on both the epidermal and dermal aspects of cutaneous wound repair may synergize, translating into the more profoundly positive effect observed by CRT treatment compared to PDGF-BB in our studies. Interestingly, CRT expression was not increased in the neoepidermis (hypertrophic) and was completely absent in the migrating epithelium and proliferating basal and suprabasal keratinocytes, which proliferated and migrated in response to CRT *in vitro*. It has been shown that calcium modulates keratinocyte proliferation and differentiation with higher concentrations promoting terminal differentiation.<sup>64</sup> A calcium gradient is shown to increase threefold from the epidermal basal layer upward to the most differentiated stratum corneum of the epidermis. Therefore, a possible explanation for the lack of CRT in the basal keratinocytes that compose the proliferative cell renewal epidermal compartment is that the presence of CRT, as a calcium-binding protein, would lead to differentiation rather than replenishment of the epidermis for epidermal healing. In contrast, the lack of CRT in the migrating epithelium is surprising in light of the importance of the calcium-dependent function of integrins in migration. Nonetheless, it is possible that the anti-CRT antibody does not recognize a particular conformation of intracellular or extracellular CRT involved in proliferation and/or migration.

Expectedly, the basal and suprabasal keratinocytes that appeared void of CRT were immunoreactive for the proliferative marker Ki-67. Consistent with the profound effect of CRT on increasing the rate of epithelial stratification, CRT induced a marked increase in the number of basal and suprabasal keratinocytes that were undergoing proliferation compared to the buffer and PDGF-BB-treated controls. The lack of Ki-67 immunoreactivity in the keratinocytes engaged in migrating over the wound bed is consistent with the fact that actively migrating cells do not proliferate. Different populations of cells throughout the wound are thus dynamically proliferating and migrating throughout the repair process. In the steroid-impaired porcine model, the apparent strong and specific effect of CRT in stimulating proliferation of the basal keratinocytes is important with respect to the potential for CRT to overcome defective or impaired healing, such as diabetic wounds. In contrast, buffer control and PDGF-BB-treated steroid-impaired wounds have equally low numbers of Ki-67 positive basal keratinocytes but there are equal numbers of immunoreactive dermal cells in the CRT and the PDGF-BB-treated wounds, expected since PDGF-BB only targets the dermis.

Consistent with the marked increase in granulation tissue formation in the CRT-treated wounds, TGF- $\beta$ 3 but not TGF- $\beta$ 1 or TGF- $\beta$ 2 was dose-dependently and dynamically highly up-regulated, particularly in cells of the dermis in the wounds 5 days after injury, which decreased by 10 days. All three mammalian isoforms of TGF- $\beta$  have been shown to be fibrogenic and induce matrix proteins, such as fibronectin and collagen<sup>49,62,65,66</sup> critical to the newly forming dermis. However, TGF- $\beta$ 3, but not the other isoforms, has been shown

to be involved in collagen gel matrix contraction (to stimulate wound contraction),<sup>67</sup> mitogenic behavior of cells,<sup>68</sup> acceleration of wound healing with decreased scarring,<sup>63,69-71</sup> induction of hyaluronan, an important component involved in neodermal formation,<sup>71,72</sup> and increasing the expression of the collagenases MMP2 and MMP9, temporally important in wound ECM remodeling.<sup>73</sup> Importantly, TGF- $\beta$ 3 is considered to be the master protein involved in "traffic control" of both epidermal and dermal cell motility during cutaneous repair.<sup>74</sup> We have recently confirmed that CRT directly and dose-dependently increases TGF- $\beta$ 3 and fibronectin protein in cultures of human dermal fibroblasts (unpublished results). In addition, TGF- $\beta$ 3 is the only isoform that has a HIF-1- $\alpha$  response element and thus, both TGF- $\beta$ 3<sup>75</sup> and CRT are proteins responsive to up-regulation under the hypoxic conditions of the wound environment. Taken together, the effect of CRT on ECM formation in neodermal remodeling is potentially escalated by its direct effect on TGF- $\beta$ 3 providing an explanation of the strong dermal influence of CRT consistent with enhanced and accelerated repair in the porcine and rat wounds.

*In vitro* we show that CRT dose-dependently stimulates proliferation of human keratinocytes and dermal fibroblasts and, to a lesser extent, human microvascular endothelial cells. In addition, the proliferative response to CRT, which was greater than the EGF and FGF controls, underscores the potent effect of CRT on cellular proliferation that we observed by Ki-67 staining of the excised wound tissue. CRT has been localized to the surface of platelets, where it binds the collagen integrin receptor  $\alpha$ 2 $\beta$ 1,<sup>76</sup> and it has been shown that CRT binds to the B $\beta$  chain of fibrinogen to mediate fibroblast proliferation.<sup>77</sup> Therefore, CRT might induce fibroblast proliferation on initial injury and fibrin clot formation during platelet granule release. Whereas CRT has been found associated within the nucleus<sup>78,79</sup> and to be integral to the stability of nuclear localization of p53, a stress response protein that blocks the cell cycle protein,<sup>80</sup> our results are the first to show that CRT directly affects cellular proliferation and are novel with respect to any effect on keratinocytes. In addition, we show that CRT induces both keratinocyte and fibroblast migration *in vitro* into the wounded area of a scratched (wounded) plate in a dose-dependent manner that surpassed the positive EGF and 5% FBS controls, respectively. Further, using a thin-membrane chamber assay, CRT similarly induces a concentration-dependent directed migration of human keratinocytes and fibroblasts with similar peaks of activity as shown for each cell type in the scratch plate assay. Keratinocytes show a magnitude greater sensitivity to CRT than fibroblasts in both the proliferative and migratory responses indicating that there are concentration-dependent cell-type specific responses to CRT. The inclusion of mitomycin C, showing little effect on migration, coupled with the results obtained with the chamber assay, ensure that the wound closure observed in the scratch plate assay is not due to cellular proliferation. As migration of keratinocytes over the wound is essential for wound resurfacing and the migration of fibroblasts into the wound is considered to be the rate-limiting step in granulation tissue formation,<sup>30,32,44</sup>

the *in vitro* studies provide mechanistic support for the profound effect of CRT on wound healing *in vivo*.

Numerous reports indicate that CRT is essential for integrin-mediated calcium signaling, which regulates cell shape and adhesion/migration on substratum<sup>2,10,12</sup> as well as fibronectin matrix assembly.<sup>81</sup> CRT binds to the KXGFFKR sequence of the cytoplasmic tail of  $\alpha$  integrins and both, functions in ensuring proper protein folding and in clustering integrins in focal contacts for substratum adhesion.<sup>1,2</sup> Accordingly, overexpression of CRT increases cell-cell and cell-substratum adhesion by increasing vinculin levels and  $\beta$ -catenin/Wnt signaling.<sup>19,20</sup> Cells underexpressing CRT have increased expression of calmodulin, activated CAMKII (calmodulin-dependent kinase II), and c-src, causing weak adhesion and spreading via focal contacts.<sup>18,20,82</sup> Furthermore, CRT null mouse embryo fibroblasts demonstrate decreased ability to migrate on fibronectin and laminin.<sup>17</sup> Whereas GFP-CRT expression was not localized to focal contacts, one study shows that CRT and another ER-resident protein, RAP (low-density LRP receptor-associated protein) are associated with integrin-based cellular adhesion complexes that link to the cytoskeleton, containing such signaling proteins as vinculin, talin, paxillin, focal adhesion kinase, and  $\alpha$ -actinin.<sup>83</sup> Nonetheless, our studies in which CRT induced motility/migration via an exogenous route suggests this response is a separate extracellular function of CRT that is mediated through putative receptor(s). Thus, CRT may affect integrin function related to migration by both its intracellular and extracellular mechanisms. In a coreceptor complex with LRP/CD91, by specifically interacting with the hep I domain of TSP-1 via its N-terminal sequence 19–36. CRT on the cell surface of fibroblasts and endothelial cells promotes focal adhesion disassembly for migration through both Gi-coupled signaling and PI3K-dependent ERK activation.<sup>23–25</sup> Currently, we are studying whether TSP-1/CRT, in conjunction with integrins or independently, operate to promote cellular migration in CRT-mediated wound healing *in vivo*.

Once monocytes egress from the circulation and mature into macrophages within the wound milieu, they secrete a plethora of cytokines and growth factors that function in inducing migration, proliferation, neovascularization, and extracellular matrix proteins to orchestrate the reparative process. Macrophages normally reach peak numbers between days 3 and 5 after healing.<sup>44</sup> One of the most interesting observations in our studies, unique to both the normal and cortisone-impaired CRT-treated wounds, is a more than threefold increase in the influx of macrophages into the wound bed compared to the PDGF-BB and buffer-treated wounds. Interestingly, more than 50% of these cells were sequestered within the microvasculature, suggesting that the process of macrophage recruitment by CRT is continuous, at least through 5 days of healing. The finding that CRT-treated steroid-impaired wounds contained greater numbers of macrophages than the control wounds suggests that CRT is able to overcome the significant impairment of the inflammatory response, due, in part, to decreased recruitment

of macrophages in both steroid-treated animal wound models and human patients. Thus, taken together with the ability of CRT to induce keratinocyte and fibroblast proliferation in the steroid-impaired porcine wounds, the use of CRT may have potential to aid in healing of impaired chronic and diabetic wounds. Importantly, CRT appears to have at least a dual effect on macrophage function crucial to wound repair. First, the observed emigration of macrophages into the wounds appears to not only be related to cytokine release by fibroblasts and other dermal cells but by directed migration, as we show that CRT induces concentration-dependent migration of both monocytes and macrophages in a chamber migration assay. That CRT appears to attract both monocytes and macrophages suggests its involvement in both recruiting monocytes from the circulation and the migration of macrophages throughout the wound bed. Second, CRT is shown to have an obligate role in the removal of apoptotic cells by both professional (macrophages, neutrophils, etc) and nonprofessional phagocytes (eg, fibroblasts).<sup>26</sup> As necrotic tissue/cells ranks with infection as an important deterrent to wound healing, requiring debridement to enable repair to proceed, taken together with the role of CRT in stimulating migration and proliferation of wound cells, this calcium-binding, stress-induced ER protein is thus portrayed as a pivotal protein in the repair of injured skin.

Failure to heal wounds from overwhelming injury or impaired healing, as in diabetes-induced neuropathic wounds, has become an increasingly serious global problem with significant morbidity and expense.<sup>30</sup> The healing impairment of these chronic wounds is due to the formation of biofilms, the presence of necrotic tissue, poor vascularization, and a diminished immune response. Although novel wound-healing agents, skin substitutes, and devices are continually emerging, their utility for clinical application remains limited as few chronic wounds are actually healed. Our wide-ranging studies show that topically applied CRT has the potential to serve as a multifunctional agent that targets both the epidermis and dermis for induction of diverse key aspects of tissue repair. The complementary *in vitro* experiments showing the effect of CRT on cellular migration and proliferation, two key processes that enable wound repair, provide a mechanistic explanation for the accelerated and enhanced effect observed of CRT on porcine wound repair. In companion studies, in which we used a diabetic murine model of excisional cutaneous repair,<sup>4,84</sup> we obtained the same biological effects with the identical pharmacological dose (5.0 mg/ml) of CRT on parameters of wound repair as shown herein in the porcine model. Further understanding the mechanisms of action of CRT (eg, receptors, signaling pathways, domain structure/function) on keratinocytes, fibroblasts, endothelial cells, and monocytes/macrophages from both intracellular and extracellular perspectives is important for a better understanding of the in-depth role of CRT as a stress/injury-induced protein with significant impact on a diverse range of reparative responses.

## Acknowledgments

We thank the many people within Vanderbilt University's Immunohistochemistry Core who provided expert technical services, and Christine D'Aquino-Ardalan for assistance in preparation of the figures.

## References

- Johnson S, Michalak M, Opas M, Eggleton P: The ins and outs of calreticulin: from the ER lumen to the extracellular space. *Trends Cell Biol* 2001, 11:122–129
- Bedard K, Szabo E, Michalak M, Opas M: Cellular functions of endoplasmic reticulum chaperones calreticulin, calnexin, and ERp57. *Int Rev Cytol* 2005, 245:91–121
- Sezestakowska D, Szabo E, Eggleton P, Opas M, Young P: Seventh International Workshop on Calreticulin, Niagara Falls, Canada: The complexities of calreticulin from folding to disease prevention and therapeutic application. *Calcium Binding Proteins* 2006, 1:135–139
- Gold LI, Rahman M, Blechman KM, Greives MR, Churgin S, Michaels J, Callaghan MJ, Cardwell NL, Pollins AC, Michalak M, Siebert JW, Levine JP, Gurtner GC, Nanney LB, Galiano RD, Cadacio CL: Overview of the role for calreticulin in the enhancement of wound healing through multiple biological effects. *J Invest Dermatol Symp Proc* 2006, 11:57–65
- Michalak M, Corbett EF, Mesaali N, Nakamura K, Opas M: Calreticulin: one protein, one gene, many functions. *Biochem J* 1999, 344:281–292
- Conway EM, Liu L, Nowakowski B, Steiner-Mosonyi M, Ribeiro SP, Michalak M: Heat shock-sensitive expression of calreticulin: in vitro and in vivo up-regulation. *J Biol Chem* 1995, 270:17011–17016
- Boraldi F, Annovi G, Carraro F, Naldini A, Tiozzo R, Sommer P, Quaglino D: Hypoxia influences the cellular cross-talk of human dermal fibroblasts: a proteomic approach. *Biochim Biophys Acta* 2007
- Hopf HW, Rollins MD: Wounds: an overview of the role of oxygen. *Antiox Redox Signal* 2007, 9:1183–1192
- Malda J, Klein TJ, Upton Z: The roles of hypoxia in the in vitro engineering of tissues. *Tissue Eng* 2007, 13:2153–2162
- Coppolino MG, Woodside MJ, Demareux N, Grinstein S, St-Arnaud R, Dedhar S: Calreticulin is essential for integrin-mediated calcium signalling and cell adhesion. *Nature* 1997, 386:843–847
- Kwon MS, Park CS, Choi K, Ahn J, Kim Ji, Eom SH, Kaufman SJ, Song WK: Calreticulin couples calcium release and calcium influx in integrin-mediated calcium signaling. *Mol Biol Cell* 2000, 11:1433–1443
- Coppolino MG, Dedhar S: Bi-directional signal transduction by integrin receptors. *Int J Biochem Cell Biol* 2000, 32:171–188
- McDonnell JM, Jones GE, White TK, Tanzer ML: Calreticulin binding affinity for glycosylated laminin. *J Biol Chem* 1996, 271:7891–7894
- White TK, Zhu Q, Tanzer ML: Cell surface calreticulin is a putative mannoside lectin which triggers mouse melanoma cell spreading. *J Biol Chem* 1995, 270:15926–15929
- Corbett EF, Michalak KM, Oikawa K, Johnson S, Campbell ID, Eggleton P, Kay C, Michalak M: The conformation of calreticulin is influenced by the endoplasmic reticulum luminal environment. *J Biol Chem* 2000, 275:27177–27185
- Fadel MP, Dziak E, Lo CM, Ferrier J, Mesaali N, Michalak M, Opas M: Calreticulin affects focal contact-dependent but not close contact-dependent cell-substratum adhesion. *J Biol Chem* 1999, 274:15085–15094
- Rauch F, Prud'homme J, Arabian A, Dedhar S, St-Arnaud R: Heart, brain, and body wall defects in mice lacking calreticulin. *Exp Cell Res* 2000, 256:105–111
- Szabo E, Papp S, Opas M: Differential calreticulin expression affects focal contacts via the calmodulin/CaMK II pathway. *J Cell Physiol* 2007, 213:269–277
- Opas M, Szewczenko-Pawlikowski M, Jass GK, Mesaali N, Michalak M: Calreticulin modulates cell adhesiveness via regulation of vinculin expression. *J Cell Biol* 1996, 135:1913–1923
- Fadel MP, Szewczenko-Pawlikowski M, Leclerc P, Dziak E, Symonds JM, Blaschuk O, Michalak M, Opas M: Calreticulin affects beta-catenin-associated pathways. *J Biol Chem* 2001, 276:27083–27089
- Barker TH, Grenett HE, MacEwen MW, Tilden SG, Fuller GM, Settleman J, Woods A, Murphy-Ullrich J, Hagood JS: Thy-1 regulates fibroblast focal adhesions, cytoskeletal organization and migration through modulation of p190 RhoGAP and Rho GTPase activity. *Exp Cell Res* 2004, 295:488–496
- Goicoechea S, Orr AW, Pallero MA, Eggleton P, Murphy-Ullrich JE: Thrombospondin mediates focal adhesion disassembly through interactions with cell surface calreticulin. *J Biol Chem* 2000, 275:36358–36368
- Goicoechea S, Pallero MA, Eggleton P, Michalak M, Murphy-Ullrich JE: The anti-adhesive activity of thrombospondin is mediated by the N-terminal domain of cell surface calreticulin. *J Biol Chem* 2002, 277:37219–37228
- Orr AW, Elzie CA, Kucik DF, Murphy-Ullrich JE: Thrombospondin signaling through the calreticulin/LDL receptor-related protein co-complex stimulates random and directed cell migration. *J Cell Sci* 2003, 116:2917–2927
- Orr AW, Pallero MA, Murphy-Ullrich JE: Thrombospondin stimulates focal adhesion disassembly through Gi- and phosphoinositide 3-kinase-dependent ERK activation. *J Biol Chem* 2002, 277:20453–20460
- Gardai SJ, McPhillips KA, Frasca SC, Janssen WJ, Starefeldt A, Murphy-Ullrich JE, Bratton DL, Oldenborg PA, Michalak M, Henson PM: Cell-surface calreticulin initiates clearance of viable or apoptotic cells through trans-activation of LRP on the phagocyte. *Cell* 2005, 123:321–334
- Ogden CA, deCathelineau A, Hoffmann PR, Bratton D, Ghebrehwet B, Fadok VA, Henson PM: C1q and mannose binding lectin engagement of cell surface calreticulin and CD91 initiates macropinocytosis and uptake of apoptotic cells. *J Exp Med* 2001, 194:781–795
- Burns K, Helgason CD, Bleackley RC, Michalak M: Calreticulin in T-lymphocytes. Identification of calreticulin in T-lymphocytes and demonstration that activation of T cells correlates with increased levels of calreticulin mRNA and protein. *J Biol Chem* 1992, 267:19039–19042
- Obeid M, Tesniere A, Ghiringhelli F, Fimia GM, Apetoh L, Perfettini JL, Castedo M, Mignot G, Panaretakis T, Casares N, Metivier D, Larochette N, van Ender P, Ciccosanti F, Piacentini M, Zitvogel L, Kroemer G: Calreticulin exposure dictates the immunogenicity of cancer cell death. *Nat Med* 2007, 13:54–61
- Clark RA, Ghosh K, Tonnesen MG: Tissue engineering for cutaneous wounds. *J Invest Dermatol* 2007, 127:1018–1029
- Clark RA: Wound repair. *Curr Opin Cell Biol* 1989, 1:1000–1008
- Gailit J, Clark RA: Wound repair in the context of extracellular matrix. *Curr Opin Cell Biol* 1994, 6:717–725
- Burd DA, Greco RM, Regauer S, Longaker MT, Siebert JW, Garg HG: Hyaluronan and wound healing: a new perspective. *Br J Plast Surg* 1991, 44:579–584
- Bakshandeh N, Siebert JW, Cabrera RC, Eidelman Y, Longaker M, Freund RW, Garg HG: Isolation and partial characterization of hyaluronan-protein-collagen complex (HA-PC) from fetal sheep skin of different gestational ages. *Biochem Int* 1992, 28:843–851
- Cabrera RC, Siebert JW, Eidelman Y, Gold LI, Longaker MT, Garg HG: The in vivo effect of hyaluronan associated protein-collagen complex on wound repair. *Biochem Mol Biol Int* 1995, 37:151–158
- Bennett LL, Rosenblum RS, Perlov C, Davidson JM, Barton RM, Nanney LB: An in vivo comparison of topical agents on wound repair. *Plast Reconstr Surg* 2001, 108:675–687
- Sullivan TP, Eaglstein WH, Davis SC, Mertz P: The pig as a model for human wound healing. *Wound Repair Regen* 2001, 9:66–76
- Guo L, Groenendyk J, Papp S, Dabrowska M, Knoblach B, Kay C, Parker JM, Opas M, Michalak M: Identification of an N-domain histidine essential for chaperone function in calreticulin. *J Biol Chem* 2003, 278:50645–50653
- Levine JH, Moses HL, Gold LI, Nanney LB: Spatial and temporal patterns of immunoreactive transforming growth factor beta 1, beta 2, and beta 3 during excisional wound repair. *Am J Pathol* 1993, 143:368–380
- Okwueze MI, Cardwell NL, Pollins AC, Nanney LB: Modulation of porcine wound repair with a transfected ErbB3 gene and relevant EGF-like ligands. *J Invest Dermatol* 2007, 127:1030–1041
- Ballas CB, Davidson JM: Delayed wound healing in aged rats is associated with increased collagen gel remodeling and contraction by skin fibroblasts, not with differences in apoptotic or myofibroblast cell populations. *Wound Repair Regen* 2001, 9:223–237
- Pelton RW, Saxena B, Jones M, Moses HL, Gold LI: Immunohisto-

- chemical localization of TGF beta 1, TGF beta 2, and TGF beta 3 in the mouse embryo: expression patterns suggest multiple roles during embryonic development. *J Cell Biol* 1991, 115:1091–1105
43. Embil JM, Papp K, Sibbald G, Tousignant J, Smiell JM, Wong B, Lau CY: Recombinant human platelet-derived growth factor-BB (becaplermin) for healing chronic lower extremity diabetic ulcers: an open-label clinical evaluation of efficacy. *Wound Repair Regen* 2000, 8:162–168
  44. Meier K, Nanney LB: Emerging new drugs for wound repair. *Expert Opin Emerg Drugs* 2006, 11:23–37
  45. Singer AJ, Clark RA: Cutaneous wound healing. *N Engl J Med* 1999, 341:738–746
  46. Leibovich SJ, Ross R: The role of the macrophage in wound repair: a study with hydrocortisone and antimacrophage serum. *Am J Pathol* 1975, 78:71–100
  47. Ogawa Y, Ksander GA, Pratt BM, Sawamura SJ, Ziman JM, Gerhardt CO, Avis PD, Murray MJ, McPherson JM: Differences in the biological activities of transforming growth factor-beta and platelet-derived growth factor in vivo. *Growth Factors* 1991, 5:57–68
  48. Ksander GA, Chu GH, McMullin H, Ogawa Y, Pratt BM, Rosenblatt JS, McPherson JM: Transforming growth factors-beta 1 and beta 2 enhance connective tissue formation in animal models of dermal wound healing by secondary intent. *Ann NY Acad Sci* 1990, 593:135–147
  49. Kinbara T, Shirasaki F, Kawara S, Inagaki Y, de Crombrugge B, Takehara K: Transforming growth factor-beta isoforms differentially stimulate proalpha2(I) collagen gene expression during wound healing process in transgenic mice. *J Cell Physiol* 2002, 190:375–381
  50. Roberts AB, Sporn MB: Transforming growth factor-beta. Edited by Clark RAF. New York, Plenum Press, 1996, pp 275–308
  51. McMullen H, Longaker MT, Cabrera RC, Sung J, Canete J, Siebert JW, Lorenz HP, Gold LI: Spatial and temporal expression of transforming growth factor-beta isoforms during ovine excisional and incisional wound repair. *Wound Repair Regen* 1995, 3:141–156
  52. Lampugnani MG: Cell migration into a wounded area in vitro. *Methods Mol Biol* 1999, 96:177–182
  53. Huang C, Liu J, Haudenschield CC, Zhan X: The role of tyrosine phosphorylation of cortactin in the locomotion of endothelial cells. *J Biol Chem* 1998, 273:25770–25776
  54. Macario AJ, Conway de Macario E: Chaperonopathies by defect, excess, or mistake. *Ann NY Acad Sci* 2007
  55. Tsutsumi S, Neckers L: Extracellular heat shock protein 90: a role for a molecular chaperone in cell motility and cancer metastasis. *Cancer Sci* 2007, 98:1536–1539
  56. Li W, Li Y, Guan S, Fan J, Cheng CF, Bright AM, Chinn C, Chen M, Woodley DT: Extracellular heat shock protein-90alpha: linking hypoxia to skin cell motility and wound healing. *EMBO J* 2007, 26:1221–1233
  57. Kovalchin JT, Wang R, Wagh MS, Azoulay J, Sanders M, Chandawarkar RY: In vivo delivery of heat shock protein 70 accelerates wound healing by up-regulating macrophage-mediated phagocytosis. *Wound Repair Regen* 2006, 14:129–137
  58. Wang JF, Olson ME, Winkfein RJ, Kulyk WM, Wright JB, Hart DA: Molecular and cell biology of porcine HSP47 during wound healing: complete cDNA sequence and regulation of gene expression. *Wound Repair Regen* 2002, 10:230–240
  59. McMurtry AL, Cho K, Young LJ, Nelson CF, Greenhalgh DG: Expression of HSP70 in healing wounds of diabetic and nondiabetic mice. *J Surg Res* 1999, 86:36–41
  60. Pierce GF, Vande Berg J, Rudolph R, Tarpley J, Mustoe TA: Platelet-derived growth factor-BB and transforming growth factor beta 1 selectively modulate glycosaminoglycans, collagen, and myofibroblasts in excisional wounds. *Am J Pathol* 1991, 138:629–646
  61. Chan RK, Liu PH, Pietramaggiore G, Ibrahim SI, Hechtman HB, Orgill DP: Effect of recombinant platelet-derived growth factor (Regranex) on wound closure in genetically diabetic mice. *J Burn Care Res* 2006, 27:202–205
  62. Sporn MB, Roberts AB: A major advance in the use of growth factors to enhance wound healing. *J Clin Invest* 1993, 92:2565–2566
  63. O'Kane S, Ferguson MW: Transforming growth factor beta-3 and wound healing. *Int J Biochem Cell Biol* 1997, 29:63–78
  64. Lansdown AB: Calcium: a potential central regulator in wound healing in the skin. *Wound Repair Regen* 2002, 10:271–285
  65. Lu L, Saulis AS, Liu WR, Roy NK, Chao JD, Ledbetter S, Mustoe TA: The temporal effects of anti-TGF-beta1, 2, and 3 monoclonal antibody on wound healing and hypertrophic scar formation. *J Am Coll Surg* 2005, 201:391–397
  66. Roberts AB, Sporn MB: Physiological actions and clinical applications of transforming growth factor-beta (TGF-beta). *Growth Factors* 1993, 8:1–9
  67. Li WY, Huang EY, Dudas M, Kaartinen V, Warburton D, Tuan TL: Transforming growth factor-beta3 affects plasminogen activator inhibitor-1 expression in fetal mice and modulates fibroblast-mediated collagen gel contraction. *Wound Repair Regen* 2006, 14:516–525
  68. Schor SL, Ellis IR, Harada K, Motegi K, Anderson AR, Chaplain MA, Keatch RP, Schor AM: A novel 'sandwich' assay for quantifying chemo-regulated cell migration within 3-dimensional matrices: wound healing cytokines exhibit distinct motogenic activities compared to the transmembrane assay. *Cell Motil Cytoskeleton* 2006, 63:287–300
  69. Wu L, Siddiqui A, Morris DE, Cox DA, Roth SI, Mustoe TA: Transforming growth factor beta 3 (TGF beta 3) accelerates wound healing without alteration of scar prominence: histologic and competitive reverse-transcription-polymerase chain reaction studies. *Arch Surg* 1997, 132:753–760
  70. Meier K, Nanney LB: Emerging new drugs for scar reduction. *Expert Opin Emerg Drugs* 2006, 11:39–47
  71. Shah M, Foreman DM, Ferguson MW: Neutralisation of TGF-beta 1 and TGF-beta 2 or exogenous addition of TGF-beta 3 to cutaneous rat wounds reduces scarring. *J Cell Sci* 1995, 108 (Pt 3):985–1002
  72. Ellis IR, Banyard J, Schor SL: Motogenic and biosynthetic response of adult skin fibroblasts to TGF-beta isoforms (-1, -2 and -3) determined by 'tissue response unit': role of cell density and substratum. *Cell Biol Int* 1999, 23:593–602
  73. Wu M, Msaeli H, Durston M, Msaeli N: Differential expression and activity of matrix metalloproteinase-2 and -9 in the calreticulin deficient cells. *Matrix Biol* 2007, 26:463–472
  74. Bandyopadhyay B, Fan J, Guan S, Li Y, Chen M, Woodley DT, Li W: A "traffic control" role for TGFbeta3: orchestrating dermal and epidermal cell motility during wound healing. *J Cell Biol* 2006, 172:1093–1105
  75. Nishi H, Nakada T, Hokamura M, Osakabe Y, Itokazu O, Huang LE, Isaka K: Hypoxia-inducible factor-1 transactivates transforming growth factor-beta3 in trophoblast. *Endocrinology* 2004, 145:4113–4118
  76. Elton CM, Smethurst PA, Eggleton P, Farndale RW: Physical and functional interaction between cell-surface calreticulin and the collagen receptors integrin alpha2beta1 and glycoprotein VI in human platelets. *Thromb Haemost* 2002, 88:648–654
  77. Gray AJ, Park PW, Broekelmann TJ, Laurent GJ, Reeves JT, Stenmark KR, Mecham RP: The mitogenic effects of the B beta chain of fibrinogen are mediated through cell surface calreticulin. *J Biol Chem* 1995, 270:26602–26606
  78. Yoon GS, Lee H, Jung Y, Yu E, Moon HB, Song K, Lee I: Nuclear matrix of calreticulin in hepatocellular carcinoma. *Cancer Res* 2000, 60:1117–1120
  79. Brunagel G, Shah U, Schoen RE, Getzenberg RH: Identification of calreticulin as a nuclear matrix protein associated with human colon cancer. *J Cell Biochem* 2003, 89:238–243
  80. Msaeli N, Phillipson C: Impaired p53 expression, function, and nuclear localization in calreticulin-deficient cells. *Mol Biol Cell* 2004, 15:1862–1870
  81. Wu C, Keightley SY, Leung-Hagesteijn C, Radeva G, Coppolino M, Goicoechea S, McDonald JA, Dedhar S: Integrin-linked protein kinase regulates fibronectin matrix assembly. E-cadherin expression, and tumorigenicity. *J Biol Chem* 1998, 273:528–536
  82. Papp S, Fadel MP, Kim H, McCulloch CA, Opas M: Calreticulin affects fibronectin-based cell-substratum adhesion via the regulation of c-Src activity. *J Biol Chem* 2007, 282:16585–16598
  83. Tran H, Pankov R, Tran SD, Hampton B, Burgess WH, Yamada KM: Integrin clustering induces kinectin accumulation. *J Cell Sci* 2002, 115:2031–2040
  84. Galiano RD, Michaels J, Dobrynsky M, Levine JP, Gurtner GC: Quantitative and reproducible murine model of excisional wound healing. *Wound Repair Regen* 2004, 12:485–492